

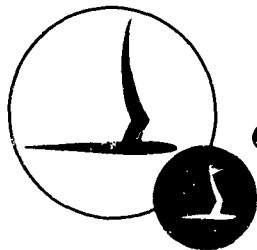
AD 43526

STUDY OF EXCITED STATES OF MOLECULAR OXYGEN BY  
MOLECULAR BEAM MAGNETIC RESONANCE  
TECHNIQUES

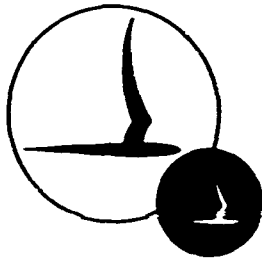
Prepared For:  
DEFENSE ATOMIC SUPPORT AGENCY  
WASHINGTON, D.C.

CLEARINGHOUSE FOR FEDERAL SCIENTIFIC AND TECHNICAL INFORMATION	
Hardcopy	Microfiche
20	6549 pp
ARCHIVE COPY	

By: Gilbert O. Brink  
Contract No. DA 49-146-XZ-483  
CAL Report No. RM-2156-P-1  
November 1966



CORNELL AERONAUTICAL LABORATORY, INC.  
OF CORNELL UNIVERSITY, BUFFALO, N. Y. 14221

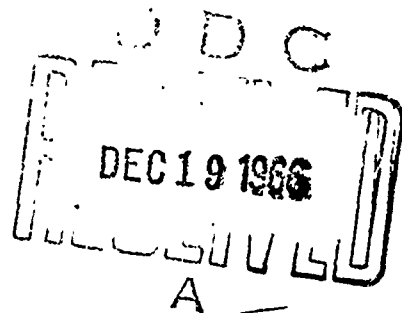


CORNELL AERONAUTICAL LABORATORY, INC.  
BUFFALO, NEW YORK 14221

STUDY OF EXCITED STATES OF MOLECULAR OXYGEN BY  
MOLECULAR BEAM MAGNETIC RESONANCE  
TECHNIQUES

CAL REPORT NO. RM-2156-P-1  
CONTRACT NO. DA 49-146-XZ-483  
NOVEMBER 1966

PREPARED FOR  
DEFENSE ATOMIC SUPPORT AGENCY  
WASHINGTON, D.C.



PREPARED BY:

*Gilbert O. Brink*

Gilbert O. Brink  
Project Engineer

APPROVED BY:

*James W. Ford*

James W. Ford, Head  
Applied Physics Department

## TABLE OF CONTENTS

Section	Page No.
LIST OF ILLUSTRATIONS . . . . .	iii
I. INTRODUCTION . . . . .	1
II. SCOPE OF PROJECT . . . . .	2
III. EXPERIMENTAL TECHNIQUE . . . . .	3
A. Molecular Beam Magnetic Resonance . . . . .	3
B. Molecular Beam Source . . . . .	7
C. Experimental Procedure. . . . .	10
IV. EXPERIMENTAL RESULTS . . . . .	14
A. $X^3 \Sigma_g^-$ Electronic Ground State of $O_2$ . . . . .	14
B. $a^1 \Delta_g$ Electronic State of $O_2$ . . . . .	14
C. $b^1 \Sigma_g^+$ State of $O_2$ . . . . .	20
D. Higher Electronic Excited States of $O_2$ . . . . .	20
E. $^3P$ Electronic Ground State of Atomic Oxygen . . . . .	20
F. $^5S$ Electronic State of Atomic Oxygen. . . . .	22
G. $^1D$ Electronic State of Atomic Oxygen. . . . .	22
H. Optical Spectra of the Discharge. . . . .	23
V. DISCUSSION . . . . .	24
VI. REFERENCES . . . . .	25
APPENDIX A - STUDY OF THE ZEEMAN EFFECT IN $O_2$ BY MOLECULAR BEAM MAGNETIC RESONANCE . . . . .	A-1
APPENDIX B - ELECTRON BOMBARDMENT MOLECULAR BEAM DETECTOR . . . . .	B-1

## LIST OF ILLUSTRATIONS

		<u>Page No.</u>
Figure 1.	Schematic of Apparatus . . . . .	5
Figure 2.	View of Molecular Beam Apparatus . . . . .	8
Figure 3.	View of Source . . . . .	9
Figure 4.	Detection System for Frequency Sweep . . . . .	11
Figure 5.	Detection System for Magnetic Field Sweep . . . . .	12
Figure 6.	Observation of ${}^1\Delta_g$ State of $O_2$ . . . . .	16
Figure 7.	Resonance Intensities as a Function of Source Pressure . . . . .	18
Figure 8.	Argon Beam Intensity vs Source Pressure . . . . .	19
Figure 9.	Resonances in Atomic Oxygen for ${}^3P$ and ${}^5S$ States	21

## I. INTRODUCTION

The purpose of this program is to investigate the effect of metastable excited states of atoms and molecules on chemical reactions that are of importance in the upper atmosphere. The majority of laboratory studies of these reactions use flowing afterglow systems in which reactive species are produced in a discharge and then allowed to react with other species in a flowing afterglow. Since these systems are usually monitored optically, it is difficult to obtain information concerning long-lived excited species directly. Many of these species contain significant energy of excitation which can alter their chemical properties markedly as compared with those of their ground states. It is desirable, therefore, to have available an experimental technique that would allow a direct assessment of the importance of these metastable states. Such a technique is that of molecular beam magnetic resonance, which permits a direct sampling of the metastable states present in the reaction system. Its preliminary application to this problem will be discussed in this report. ←

The first phase of this program is concerned with an investigation of the states of the various neutral atomic and molecular species produced by a microwave discharge in oxygen gas. The work must be limited to neutral species since ions are removed from the molecular beam by the magnet system in the apparatus. This is both a disadvantage and an advantage, since, while it prevents a direct examination of the states of the ions present in the discharge, it allows a freedom from the sampling problems associated with the extraction of charged particles from a plasma.

It is possible to predict, a priori, what the possible products of such a discharge are and the question of interest is what importance to attach to these various species. With the exception of the ionic states, the most important metastable states are the  $a^1 \Delta_g$ ,  $b^1 \Sigma_g^+$ , and  $C^3 \Delta_u$  states of  $O_2$  and the  $^1D$ ,  $^1S$ , and  $^5S^0$  states of atomic oxygen. These molecular states will be of importance not only in their ground vibrational level but also in levels having higher degrees of vibrational excitation. This preliminary work will not consider vibrational excitation; it will only be concerned with electronic and rotational excitation.

## II. SCOPE OF WORK

This report will discuss the results obtained during the first year's effort using the molecular beam magnetic resonance technique. Since this represents the first time that this apparatus has been applied to problems of this type it was necessary to expend a substantial amount of effort directed toward maximizing the detection sensitivity of the system and in obtaining data about the electronic ground state of  $O_2$ . This particular portion of the work was supported by an internal research grant from CAL.

The sensitivity of the detection system of the apparatus was increased substantially by the installation of a digital, fast-averaging signal processing computer following the electron bombardment beam detector. This modification made possible the observation of Zeeman transitions in rotational levels of  $^3\Sigma_g^- O_2$  up through the  $K = 33, J = 34$  level in a room temperature beam.

In this work a search was made for the presence of the metastable states mentioned in Section I with the exception of the  $b^1\Sigma_g^+$  and  $C^3\Delta_u$  states of  $O_2$  and the  $^1S$  state of atomic oxygen in a beam resulting from the effusion of gas from the discharge region. One of the problems associated with flowing afterglow systems is that it is generally not possible to observe the processes occurring directly in the discharge region. The molecular beam technique allows such observations to be made since the discharge may be directly sampled and the identification of the species carried out at a point external to the discharge region. Also all chemical reaction stops when the beam leaves the source tube, thus allowing an accurate sampling of the neutral composition of gas in the discharge.

The results of this search will be discussed in Section IV of this report. These results should be regarded as preliminary since it is highly probable that the concentration of a given excited species in the discharge will depend on such things as the purity of the gas and on interactions with the walls of the discharge tube. No attempts were made to purify the oxygen gas used in this work and questions concerning the effects of impurities will be left for future work.

### III. EXPERIMENTAL TECHNIQUE

#### A. Molecular Beam Magnetic Resonance

The experimental method employed in this work is that of molecular beam magnetic resonance. The general technique of molecular beams has been treated in great detail in the literature<sup>1</sup> and will not be discussed here. Only those properties of molecular beams which pertain to the present application will be discussed.

In the molecular beam magnetic resonance method the molecule in question is contained in a collision free beam and therefore is subject only to perturbations that are intentionally applied. The beam is produced in a source that populates many energy levels and thus it is possible to observe many independent resonances and many pieces of independent data can be obtained.

The signal-to-noise ratio of the beam technique is independent of frequency and resonances can be observed at low radio frequencies and weak magnetic fields. Therefore, it is possible to study the molecule under conditions such that it is subject to only very weak perturbations. This often results in a great simplification of the interpretation of the data. The resolution of the beam technique is limited by the quality of the magnetic fields used and the length of time that the molecule spends in these fields.

The molecular beam technique does have some disadvantages, the main one of which is the intensity of the resonances observed. Since the beam is neutral and cannot be focused in the sense that an ion beam can, the intensity is limited by the solid angle from the oven subtended by the magnet system. This is generally not a serious limitation, however, since beam techniques have been perfected to a high degree and the signals involved can be detected with sufficient sensitivity.

The energy of a paramagnetic molecule in a magnetic field can be written in the form

$$W = -\vec{\mu}_{\text{eff}} \cdot \vec{H} \quad (1)$$

where  $\mu_{\text{eff}}$  is the effective magnetic moment of the molecule in the magnetic field. Differentiation of equation (1) gives

$$\begin{aligned} \frac{\partial W}{\partial Z} &= -\mu_{\text{eff}} \frac{\partial H}{\partial Z} \\ &= \frac{\partial W}{\partial H} \frac{\partial H}{\partial Z} \end{aligned} \quad (2)$$

where the magnetic field is taken in the Z direction. Comparison of equations (2) shows that

$$\mu_{\text{eff}} = - \frac{\partial W}{\partial H} \quad (3)$$

Therefore the effective magnetic moment of the molecule is given by the slope of the energy levels. These slopes correspond to a magnetic moment of about one Bohr magneton.

If a paramagnetic molecule is placed in an inhomogeneous magnetic field it will experience a force given by

$$F_Z = \mu_{\text{eff}} \frac{\partial H}{\partial Z} \quad (4)$$

A beam of molecules passing at right angles through such a field will be deflected and split into components corresponding to the two possible signs of  $\mu_{\text{eff}}$ . Thus a magnet of this type can be used to polarize a molecular beam and a second magnet can be used to analyze the polarized beam. This is the basis of the molecular beam magnetic resonance method.

The experimental arrangement is shown in Figure 1. The entire system is contained inside a vacuum chamber which can be evacuated to a pressure of about  $10^{-7}$  torr. The beam is produced in a source located at the origin of the coordinate system. After collimation by a slit, the beam passes into the "A" magnet which has six poles and is similar to the magnets



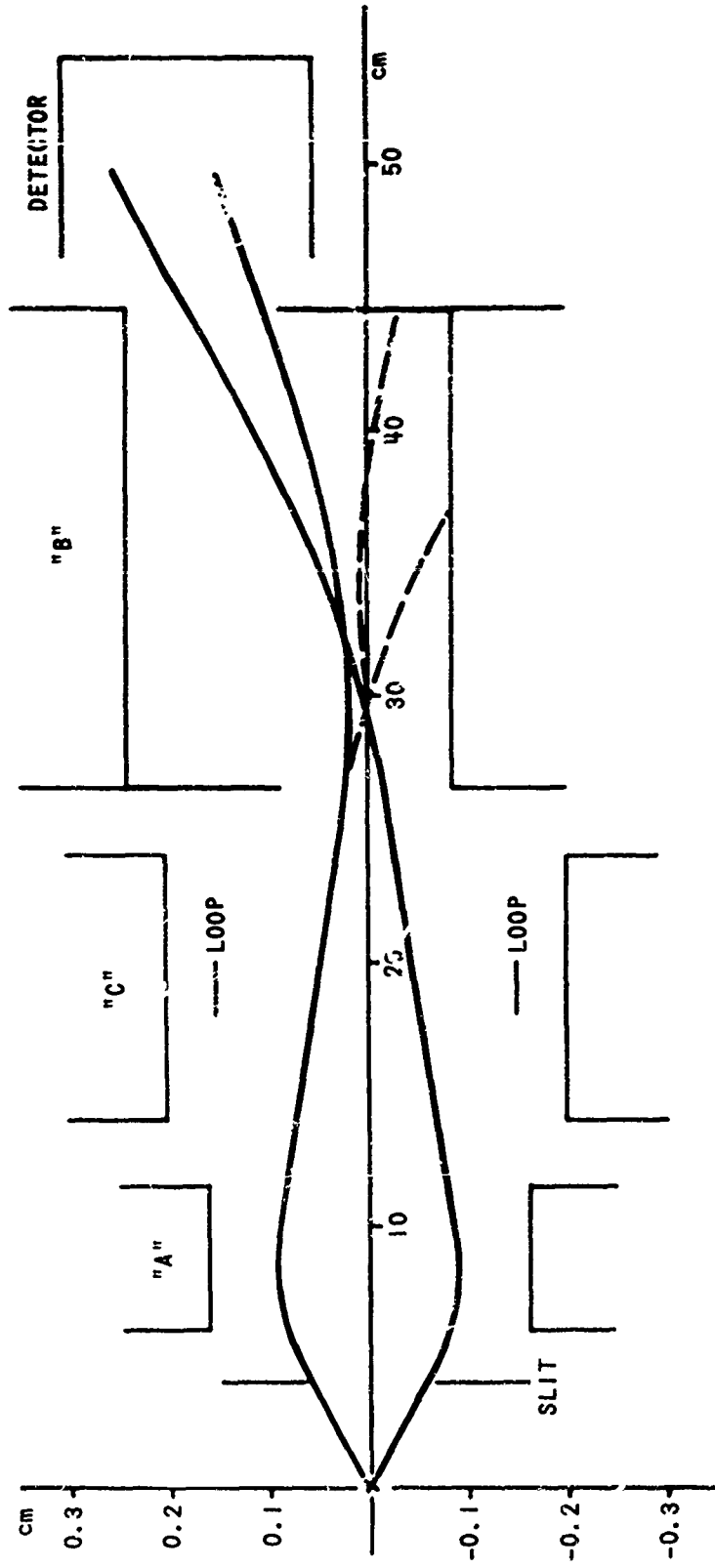


Figure 1 SCHEMATIC OF APPARATUS

used by the atomic beam group at Princeton University<sup>2</sup>. This magnet produces a field that is radially outward and has a large radial gradient. Molecules that enter the magnet with  $M_J > 0$  will be deflected toward the axis of the apparatus while molecules with  $M_J < 0$  are deflected outward. This magnet is adjusted so that most of the molecules that pass through it and can enter the entrance slit of the "B" magnet must have  $M_J > 0$ .

The "B" magnet is a two-pole magnet similar in design to a magnet used by the Princeton group<sup>2</sup> and has the property of deflecting molecules with  $M_J > 0$  downward in Figure 1, and molecules with  $M_J < 0$  upward. Thus most of the molecules entering the "B" magnet are deflected into the pole tips and cannot pass through "B" magnet exit slit.

The region between "A" and "B" magnets contains a homogeneous magnetic field produced by the "C" magnet. This region also contains a "radio frequency loop" through which the beam passes. If the frequency of the RF in the loop and the magnitude of the magnetic field are adjusted to correspond to the difference between the proper two energy levels the sign of the magnetic moment of the molecules in the beam can be reversed. Thus a molecule with  $M_J > 0$  in the "A" magnet will have  $M_J < 0$  in the "B" magnet. The molecule will now be deflected so that it passes through the exit slit of the "B" magnet, and, if a detector is placed behind this slit it will detect molecules only when they undergo a transition in the "C" field. Thus an apparatus of this kind can be used to measure the frequency and magnetic field at which transitions will take place between the energy levels of the molecules.

A typical trajectory is shown in Figure 1. Here the solid lines represent molecules that have undergone a transition. The measurement is usually made by holding the value of the "C" field constant and varying the frequency of the RF until a resonance is observed in the detector.

The resonance line width that is observed depends on the homogeneity of the "C" field and on the length of the RF loop. In the early experiments discussed here it is not desirable to have too narrow a line width because of

the search problem in locating lines. The line widths observed are usually satisfactory and can be made very small if the need arises.

In the actual apparatus the "A" and "B" magnets are permanent magnets and are located inside the vacuum envelope. This results in a less complex as well as a more stable system. The "C" magnet is a 4" electromagnet and is located outside the vacuum envelope.

The apparatus is shown in Figure 2. The system is differentially pumped so that the pressure varies from about  $10^{-6}$  Torr in the source chamber to  $10^{-9}$  Torr in the detector chamber. The most novel part of the apparatus is the beam detector which is described in Appendix B. The output of this device is amplified by a 14-stage copper-beryllium electron multiplier and the resulting signal processed by a fast averaging electronic system<sup>3</sup>. The resulting data are stored in a magnetic core memory and can be read out after the desired observation time has elapsed. This detection system has been shown to have sufficient sensitivity to detect a resonance in the  $K = 33$  rotational level of a room temperature beam of molecular oxygen<sup>4</sup>.

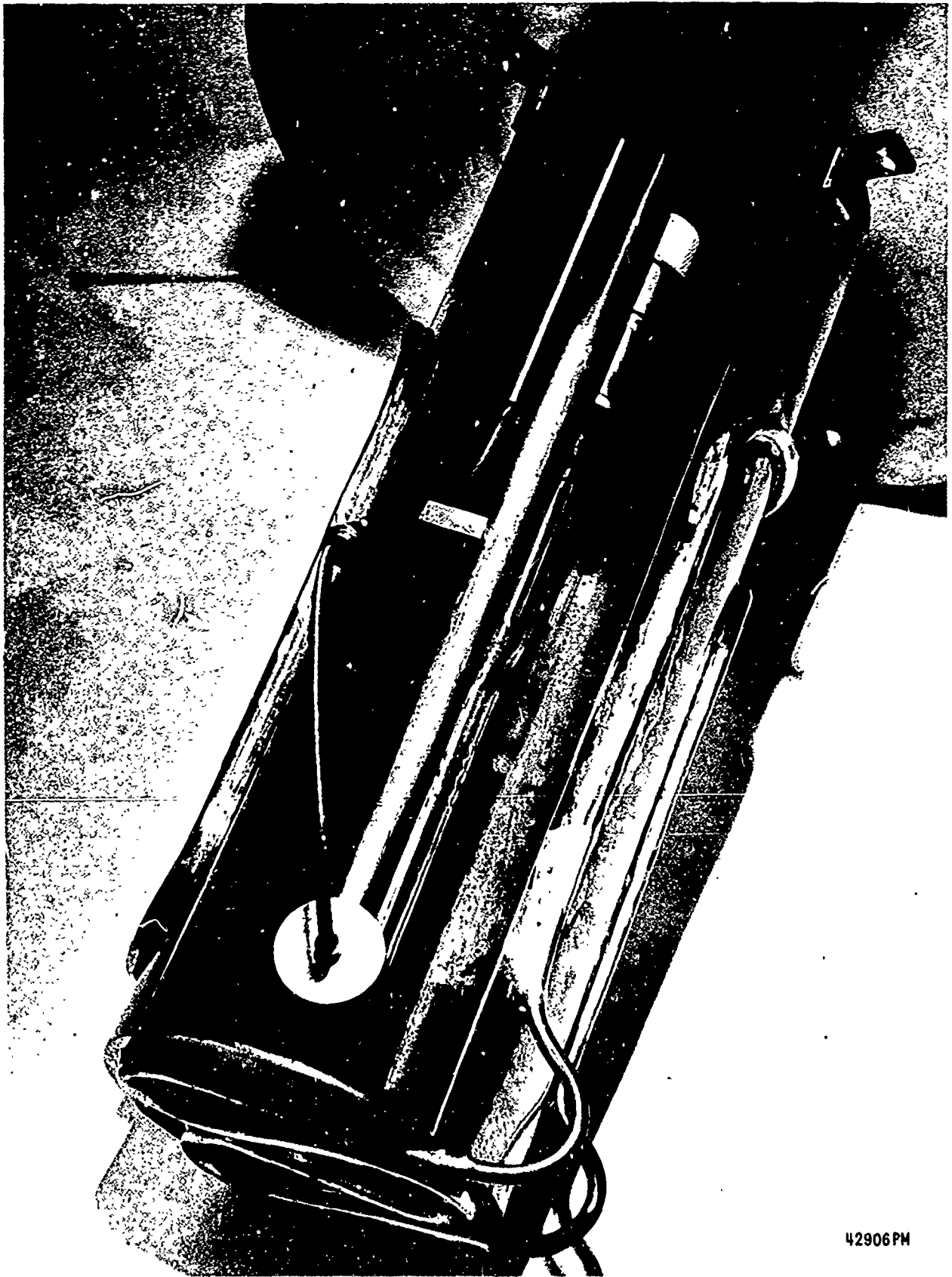
#### B. Molecular Beam Source

The molecular beam source used in this work consists of a quartz discharge tube located in a microwave cavity of a design used by Fehsenfeld et. al.<sup>5</sup>. The end of the tube is closed with the exception of a hole 0.042 cm in diameter through which the beam molecules effuse. The discharge region extends up to this hole so that this region itself is sampled by the molecular beam. The discharge tube is not cooled and is found to operate satisfactorily over the long period of time necessary for the detection of metastable states in the oxygen system.

A view of the source tube and cavity is shown in Figure 3. The outer cooled radiation shield is not used in the work herein reported. The discharge is excited by 2450 mc radiation produced by a Raytheon Microtherm. Typical operating conditions are about 50 watts input to the cavity with 3 watts reflected.



Figure 2 VIEW OF MOLECULAR BEAM APPARATUS



42906PM

Figure 3 VIEW OF SOURCE

The oxygen used in this work was tank oxygen, employed without further purification. The gas was mass analyzed, with results here presented in Table I. The optical spectrum of the discharge was observed and the results are reported in Section IV-G.

<u>Component</u>	<u>Percentage Concentration</u>
O <sub>2</sub>	98%
N <sub>2</sub>	1
H <sub>2</sub> O	1

Table I. Mass Analysis of Oxygen Gas Used.

### C. Experimental Procedure

The primary observable in an experiment of this type is a transition frequency. From a measurement of this frequency and a knowledge of the magnetic field in the resonance region of the apparatus the g-factor of the state being observed can be calculated. This g-factor is a property of a given atomic or molecular state and serves to identify that state in the beam. The species that is being observed is determined by the mass spectrometer in the beam detector.

In operation either the magnetic field or frequency is scanned in synchronization with the channel advance of the pulse height analyzer. The arrangement for frequency sweep is shown in Figure 4 and that for magnetic field sweep in Figure 5. The systems are entirely equivalent and both were used for the present work. Both systems are extremely stable, thus making possible the long search times necessary for the detection of weak signals.

was not uncommon for a search to extend for 12 - 15 hours in order to detect some of the high rotational levels of the ground state of O<sub>2</sub>.

The magnetic field in the resonance region was calibrated by the observation of a resonance of known g-factor. In early work a beam of K<sup>39</sup> was used to check the g-factor of the lower rotational levels of the  $^3\Sigma_g^-$  ground state of O<sub>2</sub>. In later work these g-factors were used to determine

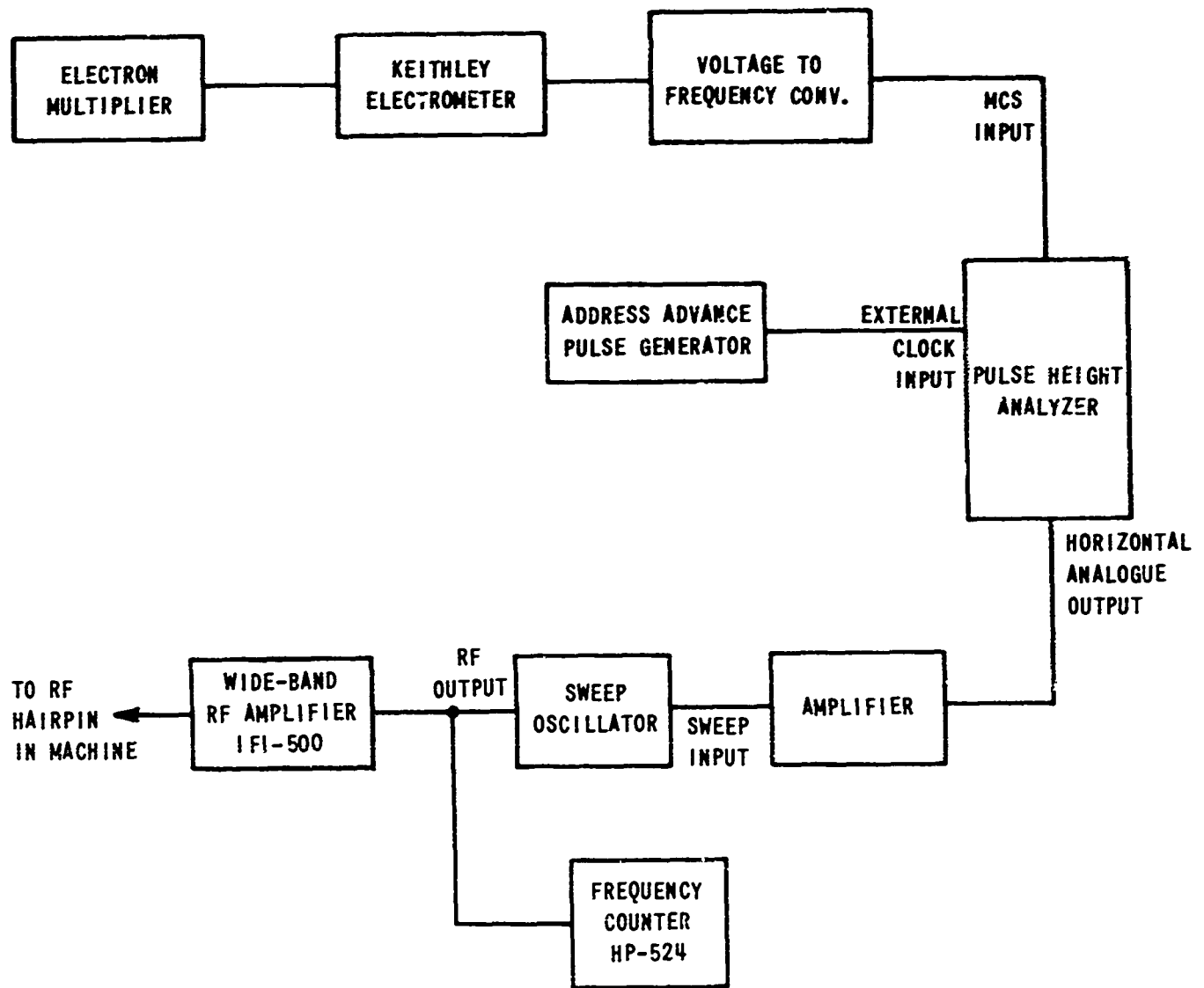


Figure 4 DETECTION SYSTEM FOR FREQUENCY SWEEP

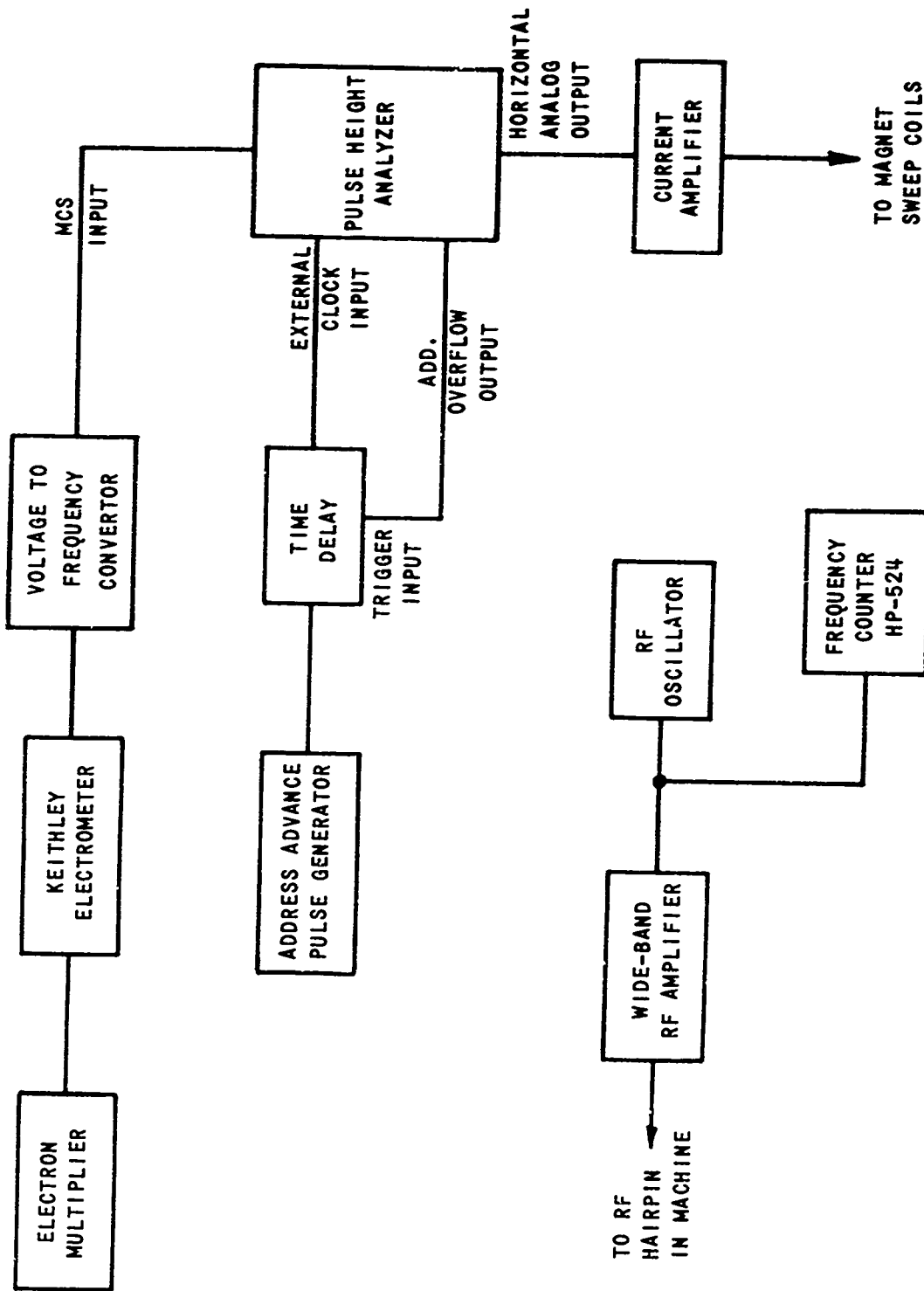


Figure 5 DETECTION SYSTEM FOR MAGNETIC FIELD SWEEP



the resonance magnetic field. This procedure is certainly justified to an accuracy necessary for the identification of the states present in the beam.

Pressure in the molecular beam source was monitored by means of a thermocouple gauge. Only approximate pressures were necessary and therefore the gauge pressures were not calibrated against an absolute standard.

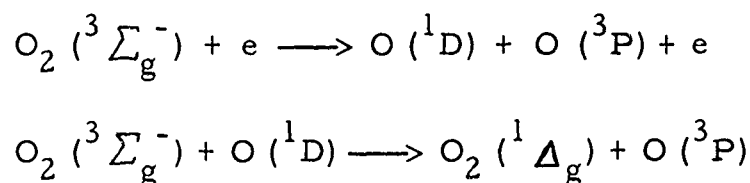
#### IV. EXPERIMENTAL RESULTS

##### A. $X^3 \Sigma_g^-$ Electronic Ground State of $O_2$

Since the most abundant component of any molecular beam containing oxygen is the  $^3 \Sigma_g^-$  state of  $O_2$  it was necessary to understand this state before any work could be done on excited states. The Zeeman effect in this state has been studied previously<sup>6, 7, 8</sup> and the work done here serves to confirm and extend the earlier work to higher rotational states. With the present apparatus it has been possible to observe rotational levels as high as  $K = 33$ ,  $J = 34$  in the ground state of  $O_2$ . Since this work is not directly related to this report it is discussed in Appendix A.

##### B. $a^1 \Delta_g$ Electronic State of $O_2$

This state has been observed previously by paramagnetic resonance in flowing afterglows<sup>9</sup> and it was the purpose of the present work to determine whether or not the state was produced directly in the discharge or was a product of reactions in the afterglow. It has been proposed that this state is a product of reactions present in the discharge and that it is produced by the following mechanism<sup>10</sup>:



If this mechanism is correct then not only should the state be observed directly in the discharge but its concentration should go as the square of the concentration of  $O_2 (^3 \Sigma_g^-)$ .

The vector model and also the high magnetic field results<sup>9</sup> predict that the lowest rotational level of this state should have a  $g$ -factor of 0.6667 and a  $J$  of 2. Since  $J$  is integral there will always be a magnetic substate with  $M_J = 0$ , and therefore it is necessary to observe either multiple quantum transitions or the transition  $M_J = +1 \longrightarrow M_J = 0$ . These two types of tran-

sitions can be selected by the placement of the beam exit slit. Attempts were first made to observe the multiple quantum transitions but these were unsuccessful, probably due to insufficient RF power in the transition region.

The  $J = 2$  level of the  ${}^1\Delta_g$  state was detected by the use of the  $\Delta M_J = -1$  transition discussed above and the results of a typical run are shown in Figure 6. Here the resonances for the  ${}^1\Delta_g$ ,  $J = 2$  and the  ${}^3\Sigma_g^-$ ,  $K = 3$ ,  $J = 4$  states are shown directly as they were read out of the pulse analyzer. In this run the mass spectrometer was tuned to mass 32, thus confirming the assignment of these states to molecular oxygen. Both of the resonances were observed simultaneously by sweeping the frequency of the RF applied to the hairpin while the magnetic field was held constant. This run required approximately 4-1/2 hours and represents about 3500 scans through the frequency region. The discharge was operated at an input power of about 50 watts with 3 watts reflected from the cavity.

The use of the observed transition frequencies and the known g-factor of the 3, 4 state which serves to calibrate the magnetic field results in the following measured g-factor of the  ${}^1\Delta_g$ ,  $J = 2$  state:

$$g({}^1\Delta_g, J = 2) = 0.75 \pm 0.02$$

This value differs from both the vector model and the high field results<sup>9</sup> by about 12%, but this is satisfactory agreement for the identification of this state as a component of the beam. The origin of this discrepancy is not clear at present, but it is not unusual for g-factors to vary with the magnetic field. Work is currently under way to remeasure the g-factor and attempt to resolve this lack of agreement. For the purposes of this report this lack of agreement is relatively unimportant. The observation of this state in the beam confirms the previous assumption, i. e., that it is produced directly in the discharge.

In order to obtain information concerning the production mechanism of the  ${}^1\Delta_g$  state in the discharge the following experiment was performed. The resonance of the  ${}^3\Sigma_g^-$ ,  $K = 3$ ,  $J = 4$  and the  ${}^1\Delta_g$ ,  $J = 2$  states were simultaneously observed and their intensities compared as a function of the

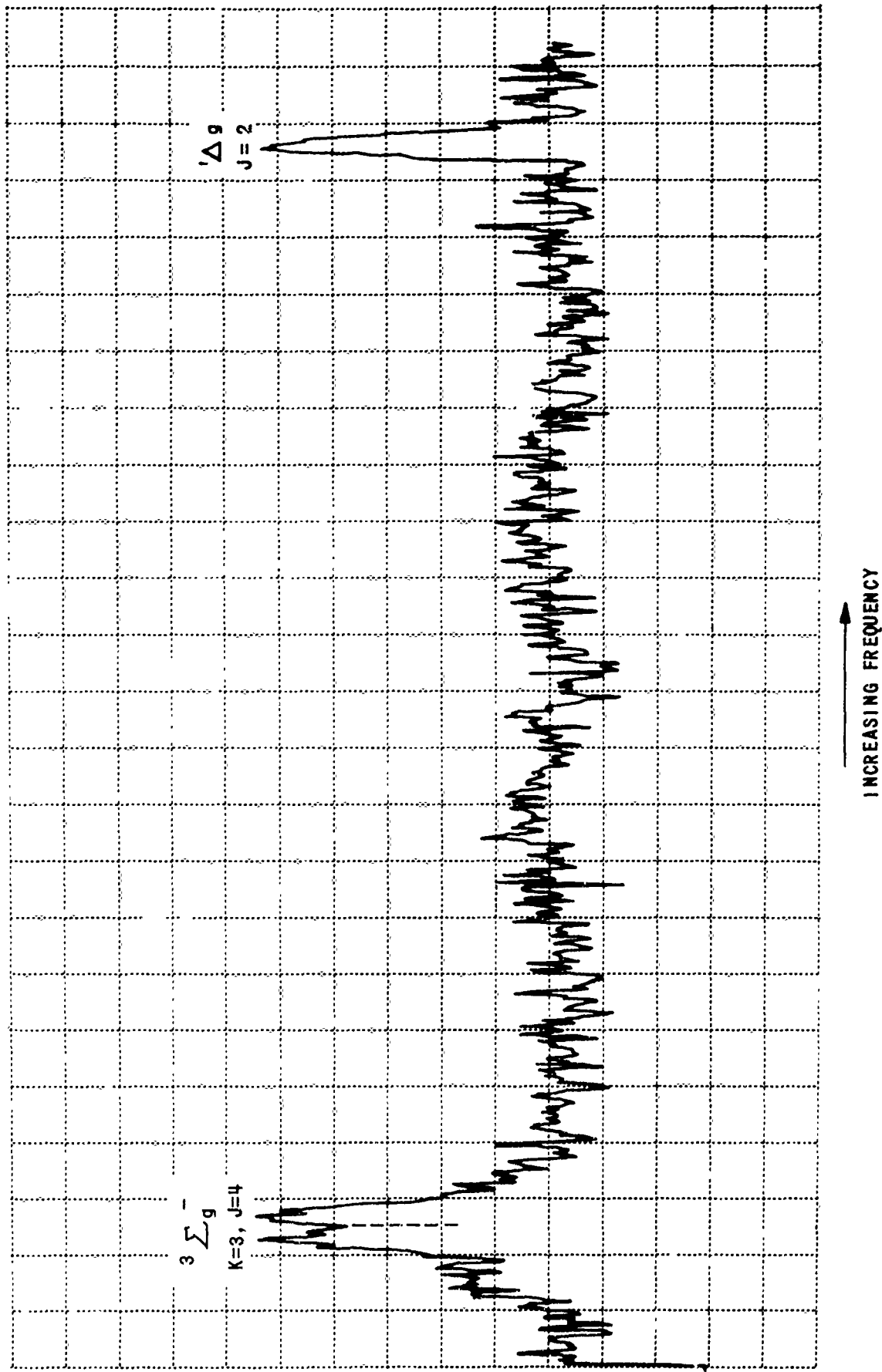


Figure 6 OBSERVATION OF  $^1\Delta_g$  STATE OF  $O_2$

gas pressure in the discharge tube. The beams machine was not disturbed during these measurements so that the intensities of the resonances should be a good measure of the relative concentrations of the species in the beam. As long as this concentration in the beam is directly proportional to the concentration in the source these results should provide a reliable measurement of the relative concentrations of these species in the discharge.

The results of these measurements are shown in Figure 7 where the observed intensity of the  $J=2$  resonance is plotted as a function of the observed intensity of the  $K=3, J=4$  resonance. The approximate pressure range over which these measurements extend is 0.76 to 1.40 Torr. This range was limited on the low side by signal intensity and on the high side by source conditions necessary for the formation of a molecular beam. Although there is considerable scatter in the data due to the weak signals involved, the data seem most consistent with a straight line through the origin rather than a quadratic curve. These data suggest that the previously proposed mechanism for the production of the  $^1\Delta_g$  state is incorrect and that the correct mechanism is one that is first order in the  $O_2(^3\Sigma_g^-)$  concentration.

The above result would be subject to criticism if the concentration of a given state in the beam were not directly proportional to the concentration of that same species in the source. In order to check on this point the source tube was filled to approximately 0.1 Torr with argon and the direct argon beam detected by placing the beam exit slit on the beam axis. A resonance was not observed; only the intensity of the direct beam was followed during the measurement. Oxygen gas was admitted to the source tube without changing the partial pressure of the argon and the intensity of the argon beam was observed as a function of the total pressure in the source tube. The results are shown in Figure 8, in which the intensity of the argon beam is plotted as a function of the total source pressure. It can be seen that the intensity of the argon beam is constant over the range from 0 to 1.4 Torr and then drops only slightly for pressures up to 2.0 Torr. This shows that the intensity of the argon beam is a good measure of the concentration of argon in this particular source tube over the entire range of pressures used in obtaining the data of Figure 7. Therefore the results of Figure 7 should be valid over the pressure range used.

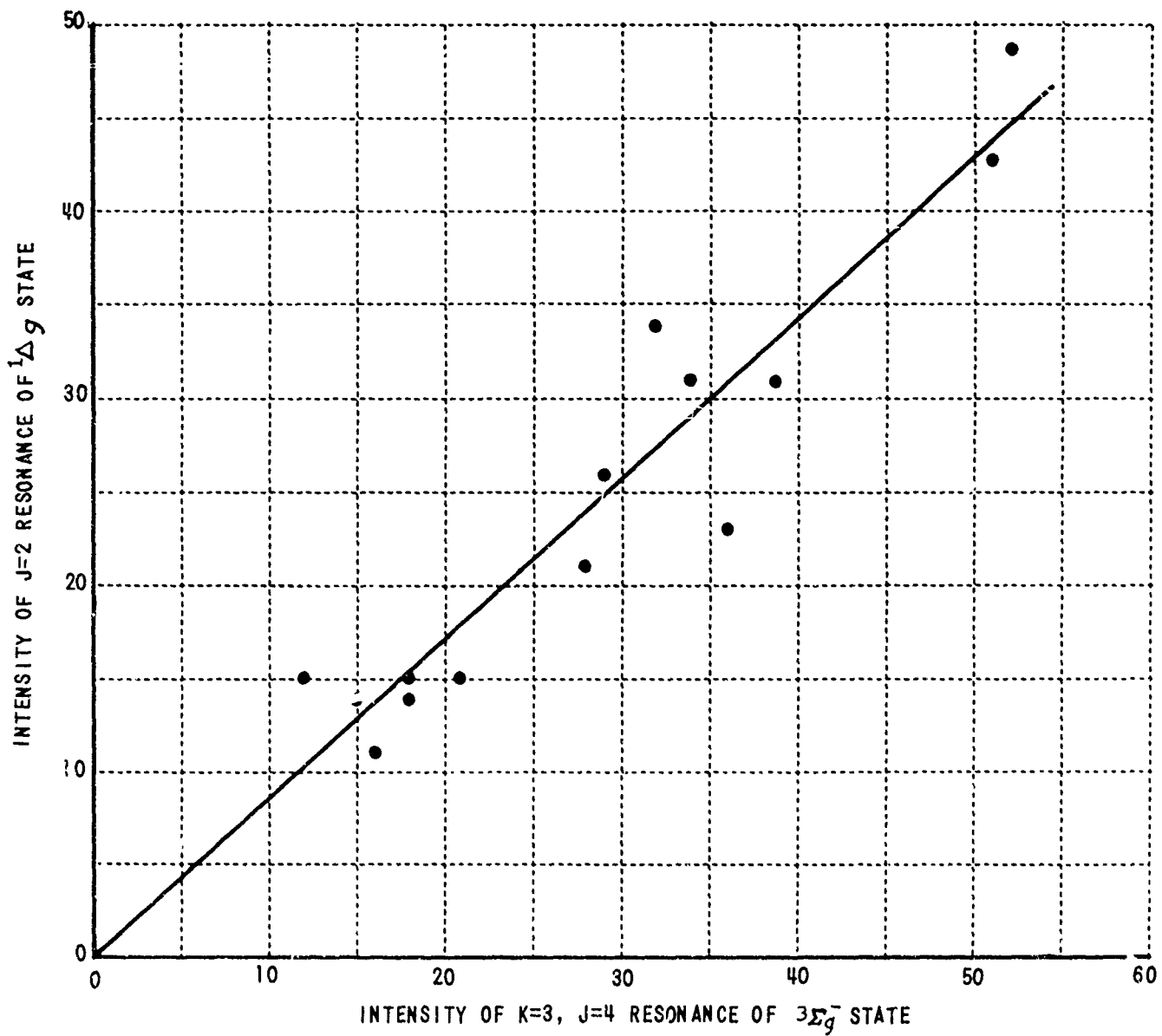


Figure 7 RESONANCE INTENSITIES AS A FUNCTION OF SOURCE PRESSURE

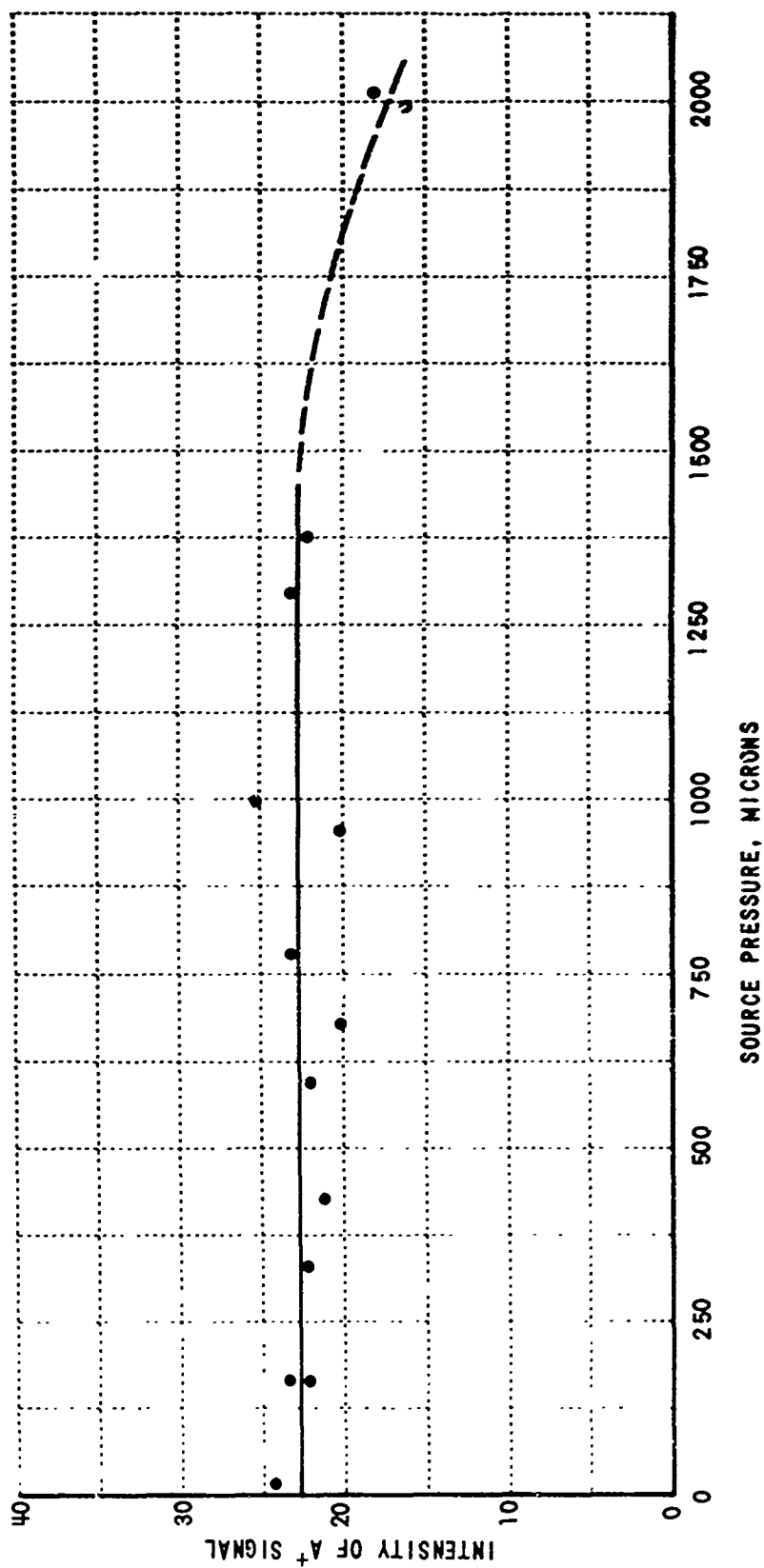


Figure 8 ARGON BEAM INTENSITY VS SOURCE PRESSURE

### C. $b^1 \Sigma_g^+$ Electronic State of $O_2$

Since this state is not paramagnetic it is not possible to observe it by means of the resonance technique being used in the current work. It may be possible, however, to observe it as a component of the direct beam and this will be attempted in the future. No data is available at present.

### D. Higher Electronic Excited States of $O_2$

The only higher metastable electronic state of  $O_2$  that may be observable by this technique is the  $C^3 \Delta_u$  state. No attempt has been made so far to observe this state among the products of the discharge. The probability of producing this state in a discharge is not great and the signals due to this state, if they are detectable at all, will be very weak. A search will be carried out for this state in the future.

### E. $^3P$ Electronic Ground State of Atomic Oxygen

The electronic ground state of atomic oxygen is the most abundant atomic state produced in the discharge. Its detection is readily accomplished even though the use of a multiple quantum transition is required because of the atom's integral J values. The state is actually a triplet that is split by the fine structure interaction in atomic oxygen. The three components of the triplet are  $^3P_2$ ,  $^3P_1$ , and  $^3P_0$  with the  $^3P_2$  state lying lowest. The  $^3P_2$  and  $^3P_1$  states both have  $g = 1.500$  and the  $^3P_0$  has  $g = 0$ . Hence only one resonance is observable with the former g-factor.

The  $^3P$  state has been observed numerous times and a typical run is shown in Figure 9. In this run the discharge was operating at about 50 watts input with 3 watts reflected from the cavity. The source pressure was about 1.5 Torr and the total run time was 115 minutes. This was a magnetic field sweep in which the RF frequency was held constant at 16.800 mc. The mass spectrometer was tuned to mass 16. The resonance is much stronger than in the molecular case due to the fewer number of states over which the available atoms must be distributed. Also the line is quite narrow due to its being a multiple quantum transition.



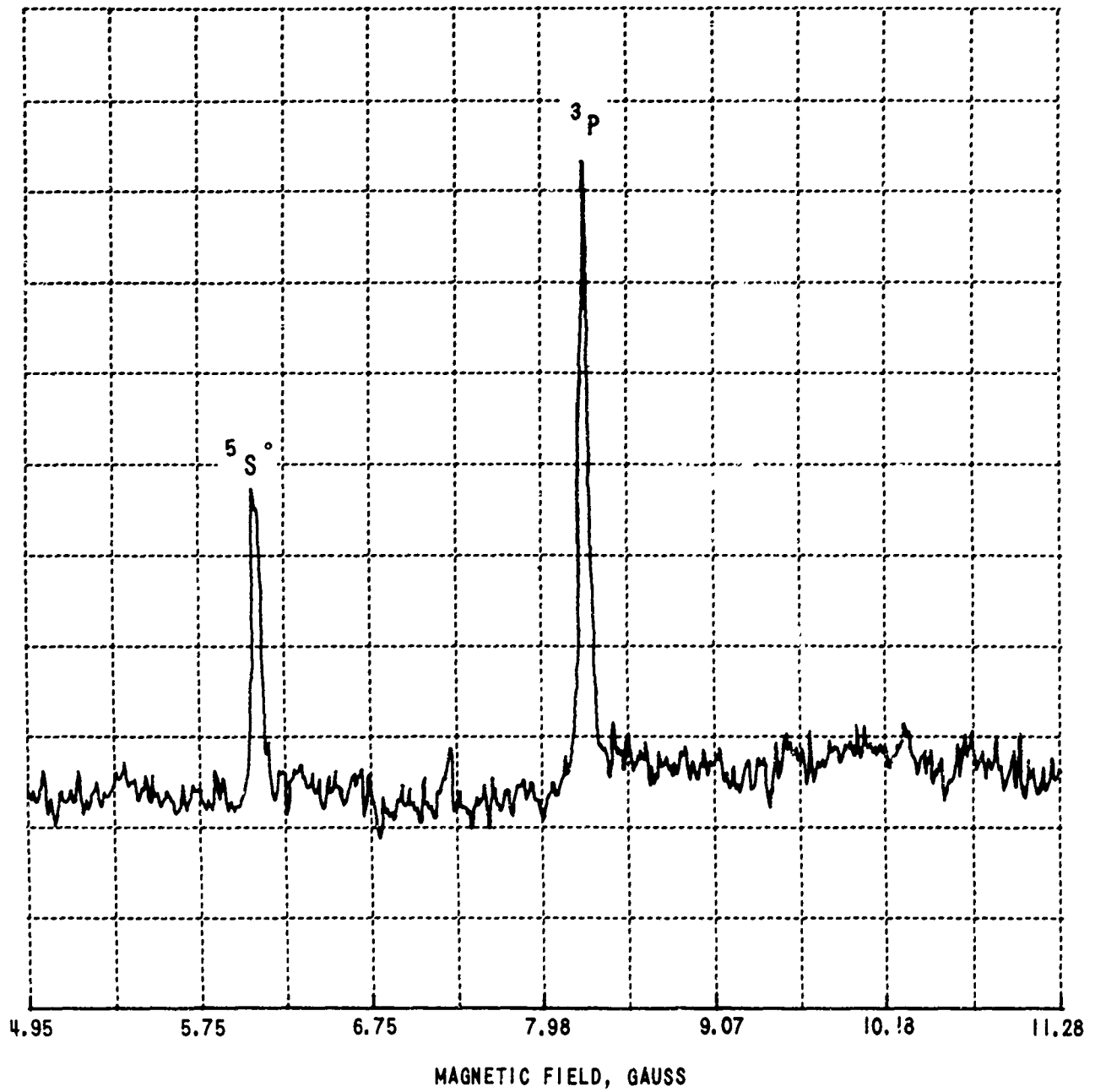


Figure 9 RESONANCES IN ATOMIC OXYGEN FOR  $^3P$  AND  $^5S$  STATES

## F. $^5S$ Electronic State of Atomic Oxygen

In runs in which the  $^3P$  state of oxygen was being observed, a second resonance was often seen with about half the intensity of the  $^3P$  state. By using the  $^3P$  state for magnetic field calibration it was determined that this second resonance had a g-factor of  $1.97 \pm 0.05$ . This resonance must, therefore, be due to an S state whose g-factor is 2.00. An examination of the energy level of atomic oxygen<sup>11</sup> shows that the only metastable S states are the  $^1S$  and a higher lying  $^5S$ . Since the g-factor of the  $^1S$  state is zero this resonance must be due to the  $^5S$  state. Optical data which will be discussed in Section IV-G bear out this assignment. A resonance in the  $^5S$  state is also shown in Figure 9.

The production of this state seems to depend strongly on the discharge conditions since it is not always seen in every discharge. It is planned to obtain further information concerning this matter in future work.

## G. $^1D$ Electronic State of Atomic Oxygen

The situation concerning this state is somewhat confused at the moment. While it is almost certainly produced in the discharge, it is so easily quenched that it may not be possible to build up a significant concentration of it in the discharge region. In a number of runs resonances have been observed with a g-factor corresponding to this state. The problem arises, however, that the g-factor of the  $^1D$  state is almost the same as that for the 1, 1 level of the  $X^3\Sigma_g^-$  state of  $O_2$ . It is possible to detect resonances in this state of  $O_2$  with the detector tuned to mass 16 by means of dissociative ionization. Hence one must be very careful in assigning a resonance to the  $^1D$  state in the presence of a large concentration of ground state  $O_2$ .

The definite identification of this state in the discharge will have to await future work. About all that can be said at present is that resonances have been observed with a g-factor corresponding to that for the  $^1D$  state of atomic oxygen. The possibility that these resonances were due to the 1, 1 rotational level of ground state of  $O_2$  can not be ruled out at this time. Experiments will be done in the near future using helium as a buffer gas, and it may be possible then to make some definite statements concerning the presence of oxygen  $^1D$  in the discharge.

#### H. Optical Spectra of the Discharge

As an aid to the interpretation of the beam data the optical spectrum of the discharge was observed simultaneously with the observation of the molecular beam. A monochromator was used as an optical spectrograph and no attempt was made to achieve resolution higher than that necessary to observe the line spectrum of atomic oxygen. The majority of the atomic oxygen lines that lie in the region from 3800 to 8500  $\text{\AA}$  were observed, as well as the band systems of  $O_2^+$  that lie in this region. In particular, the atomic oxygen lines at 3947 and 7774  $\text{\AA}$  were seen in the discharge. These lines are due to transitions from the  $4^5P$  and  $3^5P$  states to the  $3^5S^0$  state respectively. Since the  $3^5S^0$  state is forbidden to radiate to lower states, this result implies that, except for chemical effects, this state should exist in a nonzero average concentration in the gas of the discharge. This result confirms, therefore, the observation of a  $^5S$  state as a component of the beam effusing from the discharge gas.

An atomic hydrogen line at 6563  $\text{\AA}$  was also observed, indicating the presence of either hydrogen gas or water vapor in the discharge gas. The results of the mass spectroscopic analysis indicate that it is probably due to the latter.

## V. DISCUSSION

This work has resulted in the observation of one metastable state of molecular oxygen and two metastable states of atomic oxygen as well as the ground states of these species in a molecular beam produced by a microwave discharge in oxygen gas. Of these metastable states, only the  $^1\Delta_g$  state of  $O_2$  had previously been observed by means of a resonance technique<sup>9</sup>. Information about the other states has been inferred from chemical reactions occurring in flowing afterglows or from optical data. The major significance of the present work is the development of a technique for studying these states in the discharge, which allows unique identification of the species. The technique should also allow information to be obtained concerning chemical reactions involving these species in the discharge gas or in a flowing afterglow.

It is apparent from the preceding data that it will be necessary to control discharge conditions very carefully in future work. It will also be important to know the composition of the discharge gas since impurities will probably have a profound effect on the metastable states produced. These considerations are indicated by the fact that a given metastable state is not always found in the discharge even though the discharge conditions are thought to be reproducible. A good example is the  $^5S$  state, which is not always seen in the  $O_2$  discharge. When it is seen, the signals are sufficiently intense to allow very little doubt about its presence. It is possible that it is easily quenched by collision or that it is sensitive to reaction with some impurity that may be present in extremely small concentration.

It is presently planned that future work will be directed toward obtaining an understanding of the processes occurring in the discharge itself. A closer control will be maintained on the composition of the discharge gas and the effect of intentionally added impurities will be noted. It will also be necessary to closely monitor such discharge conditions as input and reflected RF power.

## VI. REFERENCES

1. N. F. Ramsey, Molecular Beams, (Oxford University Press, London, 1956).
2. M. Posner, Measurement of the Spin of Nitrogen - 13 by Atomic Beam Methods, Princeton University Technical Report NYO-2946, July 1961.
3. M. P. Klein and G. W. Barton, Jr., Rev. Sci. Instr. 34, 754 (1963).
4. Gilbert O. Brink, Bull. Am. Phys. Soc. II, 11, 711 (1966).
5. F. C. Fehsenfeld, K. M. Evenson, and H. P. Broida, Rev. Sci. Instr. 36, 294 (1965). The cavity used was design number 5.
6. M. Tinkham and M. W. P. Strandberg, Phys. Rev. 97, 951 (1955).
7. J. M. Hendrie and P. Kusch, Phys. Rev. 107, 716 (1957).
8. K. D. Bowers, R. A. Kamper and C. D. Lustig, Proc. Roy. Soc. (London) A251, 565 (1959).
9. Arnold M. Falick, Bruce H. Mahan, and Rollie J. Myers, Jour. Chem. Phys. 42, 1837 (1965).
10. E. A. Ogryzlo, Discussion of the Faraday Society, 37, 218 (1964).
11. Charlotte E. Moore, Atomic Energy Levels, NBS Circular No. 467, June 15, 1949.

## APPENDIX A

### STUDY OF THE ZEEMAN EFFECT IN O<sub>2</sub> BY MOLECULAR BEAM MAGNETIC RESONANCE \*

Gilbert O. Brink

Cornell Aeronautical Laboratory, Inc.  
Buffalo, New York

As part of a program for the study of paramagnetic molecules by the technique of molecular beam magnetic resonance the Zeeman effect in the electronic ground state of O<sub>2</sub> is being investigated. This state has received considerable previous attention<sup>1, 2, 3</sup> and the present work was undertaken in order to extend the earlier data to higher rotational levels. The present work has resulted in the observation of all rotational states up to and including that for K = 33 in a room temperature beam of O<sub>2</sub>.

The apparatus is shown in the first slide. It is a flop-in type apparatus utilizing a differentially pumped vacuum system with the pressure varying from 10<sup>-6</sup> Torr in the oven chamber to 10<sup>-9</sup> Torr in the detector chamber. The beam is detected by means of an electron bombardment ionizer and mass spectrometer which has been described in the literature<sup>4</sup>. The output of the mass spectrometer is observed by an electron multiplier and the resulting signal time averaged by a digital fast-averaging system.

The next slide shows the resonance that was observed in the K = 1 state. If the states are labeled by the notation (K, J) the lines correspond to the (1, 2) and the (1, 1) states respectively. The position at which the (3, 2) resonance would have appeared is shown on the slide. This line was not observed and theory predicts that it should not be observable.

The next slide shows resonances in the next few rotational levels. Note in particular that the (5, 4) resonance is weak compared with the (5, 6) resonance while the (7, 6) resonance is stronger than that for the (7, 8) state. This is not an RF power effect and its cause will be discussed later. The theory predicts that resonances should only be observable in the (K, K) and the (K, K+1) states of each spin triplet.

---

\* Presented at the APS Meeting, Mexico City, 29 - 31 August, 1966.

The fourth slide shows the next series of rotational levels. Note that (9, 10) is weak compared with (9, 8). Since the g-factor for the (11, 12) and the (3, 3) states are the same they are not resolved in the present work. The wing of the (13, 12) resonance is shown.

The fifth slide shows still higher rotational transitions. Note, in particular, that the (13, 14) resonance is strong while that for the (15, 16) state is weak. Again, that for (17, 18) is strong while that for (19, 20) is unobservable and that for (21, 22) is strong. The small shoulder on the lines are probably due to multiple quantum transition. The (11, 12) and (3, 3) resonances are beginning to split at this field.

The next slide shows the highest rotational states observed. Here the intensity pattern approximately repeats up to the highest state observed, the (33, 34) state. This data represents a total scan time of 600 minutes and approximately 9000 scans through the frequency region.

The data seems to be best interpreted by means of the energy level diagram shown in the next slide for  $K = 5$ . It is apparent from this diagram that resonances should only be observable in the state (5, 6). Since all of the levels for the (5, 4) state have the same slope at high magnetic fields a resonance in this state should not be focusable in an apparatus of the flop-in type. This same pattern repeats in the higher rotational states with the only complication being the increasing multiplicity as  $K$  and  $J$  increase. Therefore one would not expect to see resonances in states of the type  $(K, K-1)$ .

In order to explain the observation of these forbidden resonances it seems necessary to assume the occurrence of a nonresonance transition of the type  $\Delta J = \pm 2$ ,  $\Delta M = 0$  in the region between either the A and C or the C and B magnets. This is not the usual Majorana type transition in which  $\Delta J = 0$ ,  $\Delta M = \pm 1$  and which is produced by a rotating magnetic field intensity seen by the molecule as it passes through the magnet system.

It can be seen from the slide that the  $J = 6, M = -4$  and  $J = 4, M = -4$  levels approach each other quite closely at a field of about 175 gauss. In fact, they approach to within 2 mc of one another. Assume, therefore, that a molecule enters the A magnet in the (6, -4) state. On leaving the

A and entering the C magnet the molecule must move along the energy level curve shown. Suppose, however, that in the region between these magnets the molecule should undergo a transition to the (4, -4) level. The molecule could now undergo an RF transition in the C magnet to the (4, -3) level and enter the B magnet in that level. This would correspond to an observable resonance in the  $K = 5, J = 4$  state. The probability of observing such a resonance would depend on the closeness of approach of the  $M = -4$  states in the region between the magnets.

These considerations can be used to explain the observation of the other unobservable resonances in the higher rotational states. As far as I know, nonresonance transitions of this type have not been previously observed - probably because in the usually-studied case of atoms the levels do not approach closely enough to make the transition probability observable. If this situation turns out to be common in paramagnetic molecules it will be useful in increasing the number of observable transitions in a flop-in apparatus.

The work will be extended in the near future to the observation of RF transition between the states of the same  $M$  at fields in the region of the closest approach of these levels. This will allow a precise determination of these minimum separations for comparison with the theory of Tinkham and Strandberg.

---

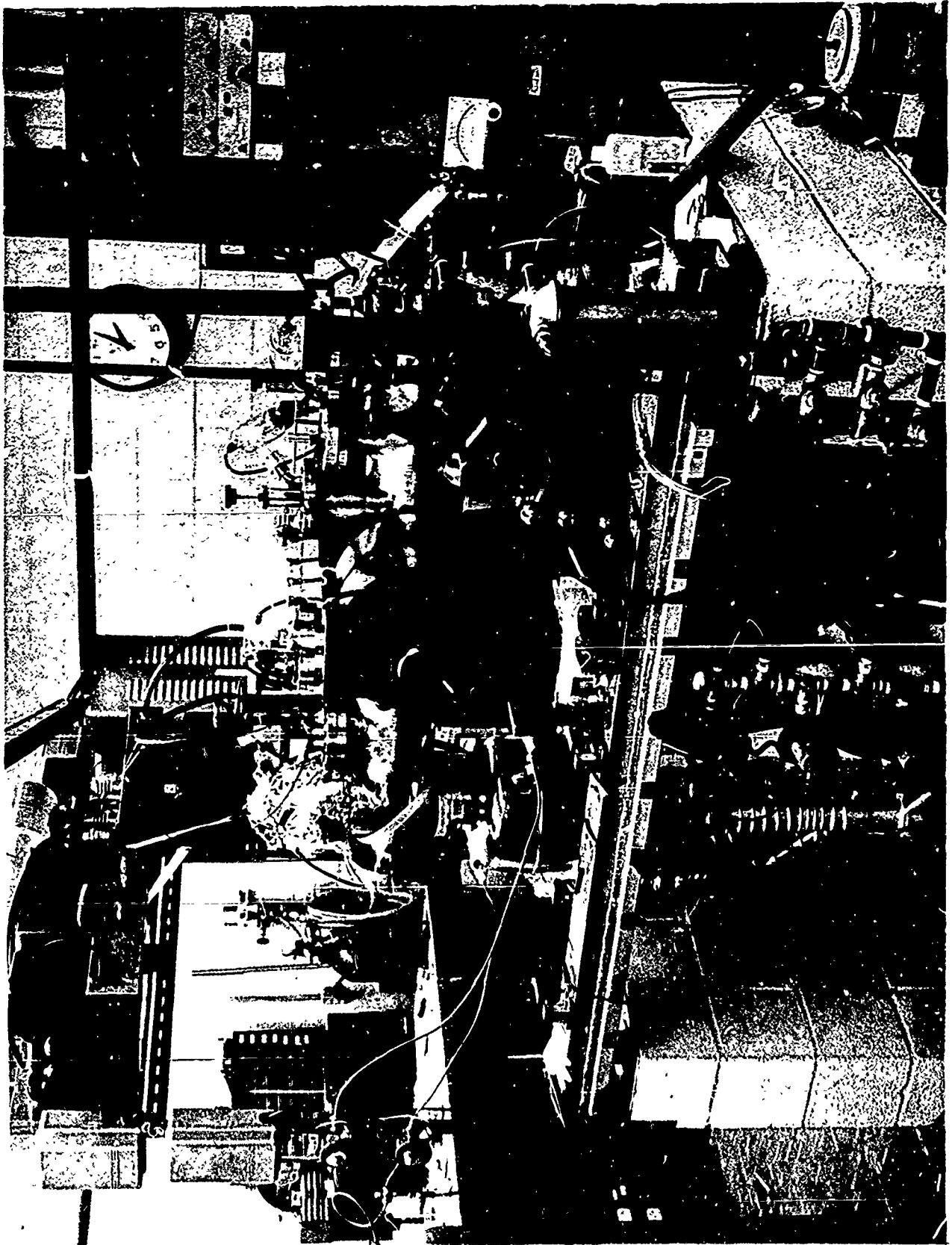
<sup>1</sup>M. Tinkham and M. W. P. Strandberg, Phys. Rev. 97, 951 (1955)

<sup>2</sup>J. M. Hendrie and P. Kusch, Phys. Rev. 107, 716 (1957)

<sup>3</sup>K. S. Bowers, R. A. Kamper and C. D. Lustig, Proc. Roy. Soc. 215A, 565 (1959)

<sup>4</sup>G. O. Brink, Rev. Sci. Instr., 37, 857 (1966)

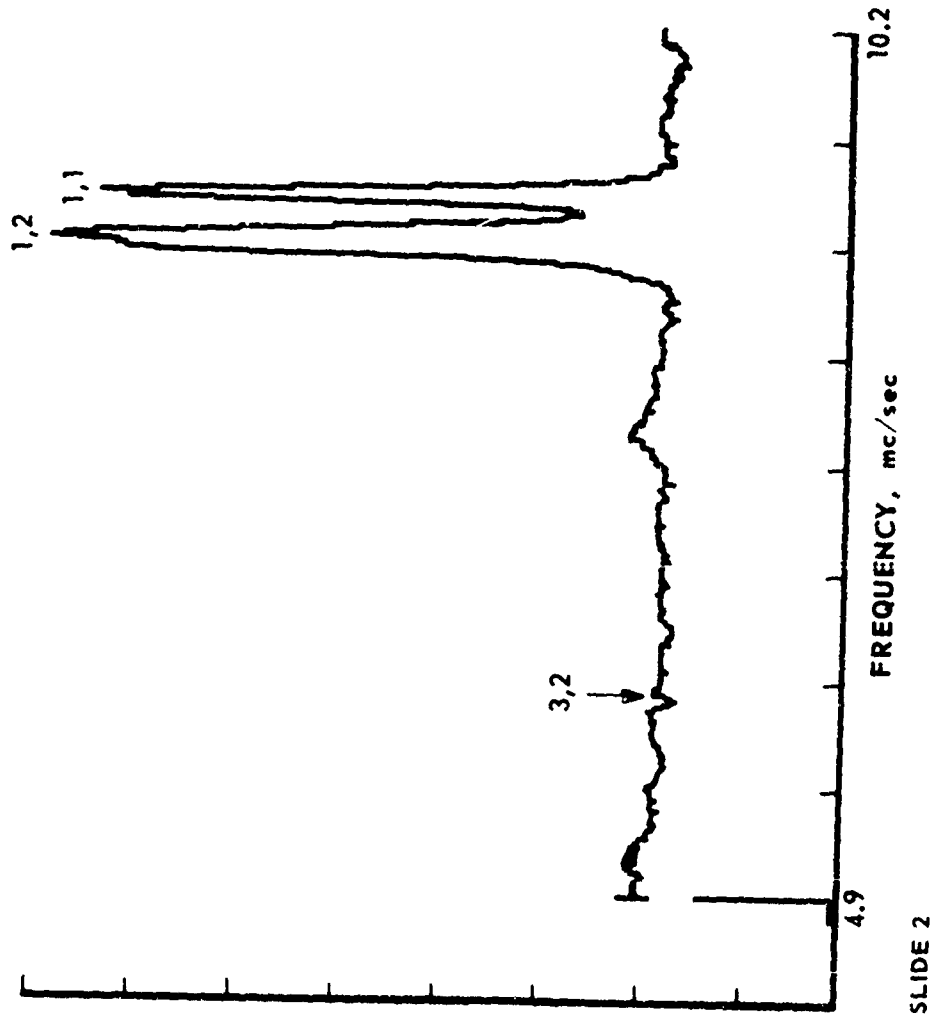




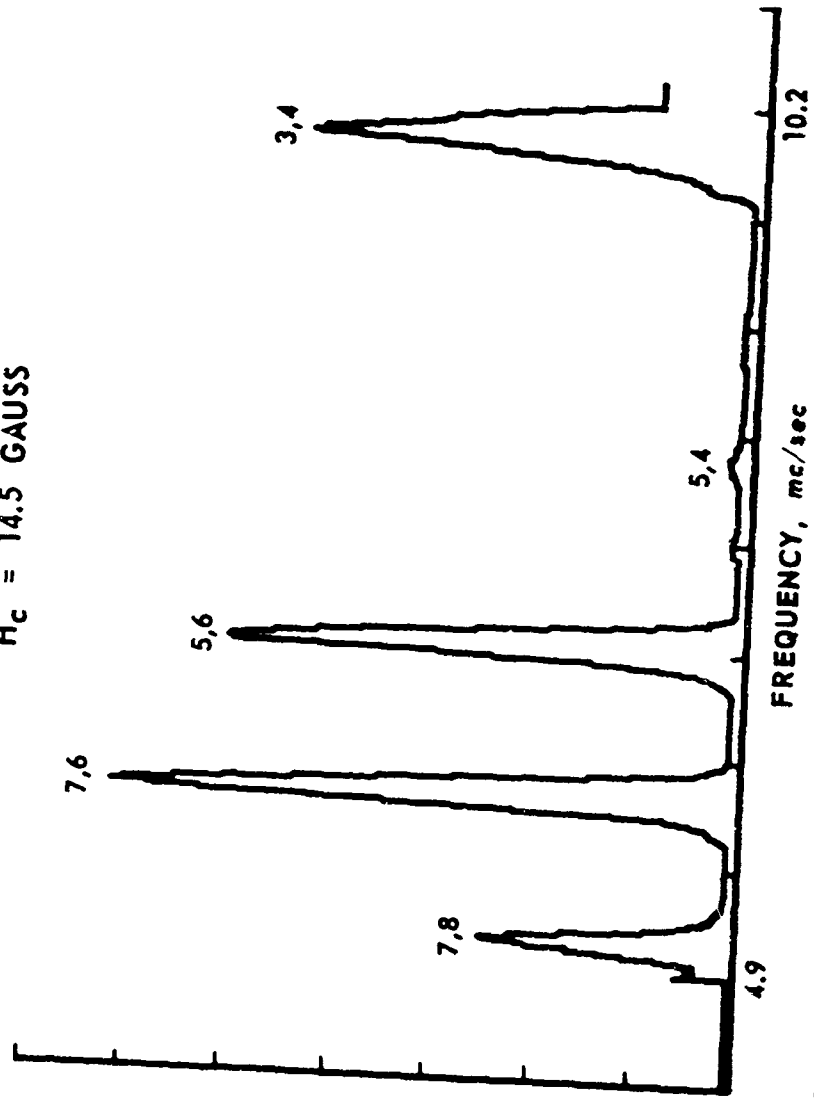
SLIDE 1

ZEEKMAN TRANSITIONS IN O<sub>2</sub>

H<sub>c</sub> = 6.6 GAUSS



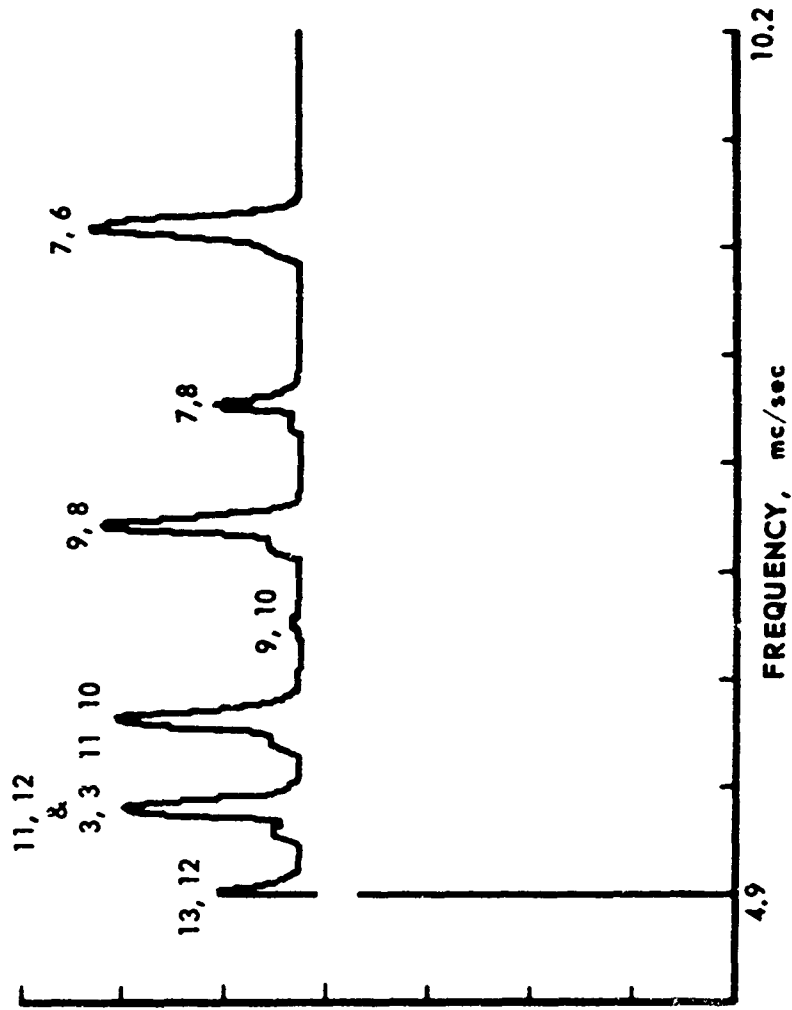
ZEEMAN TRANSITIONS IN O<sub>2</sub>  
H<sub>c</sub> = 14.5 GAUSS



SLIDE 3

ZEEMAN TRANSITIONS IN O<sub>2</sub>

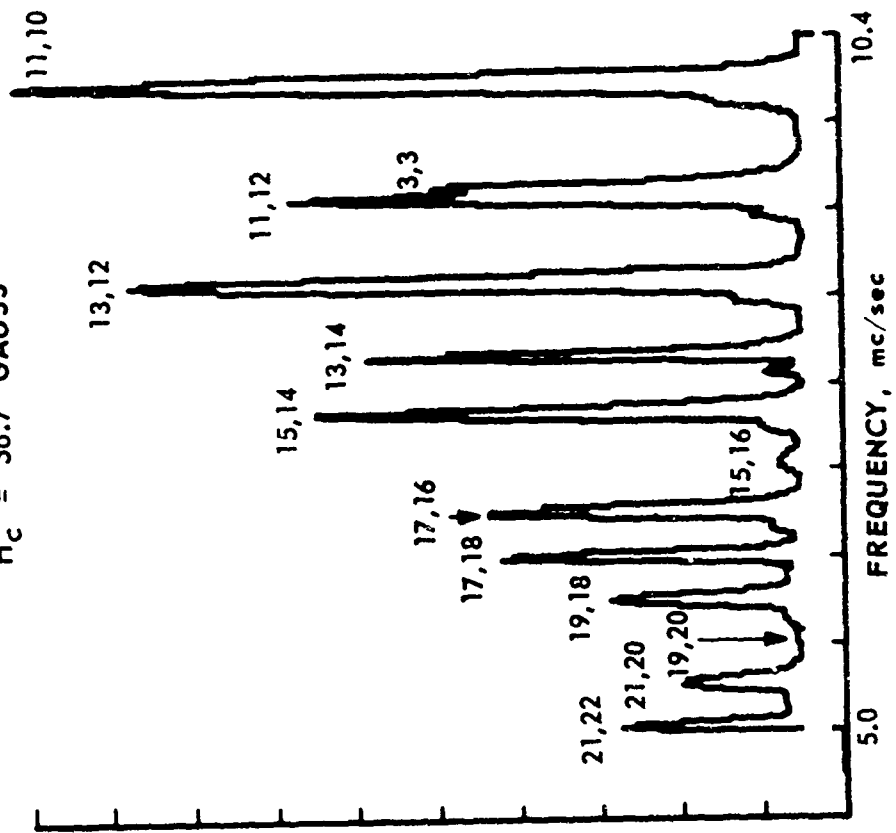
H<sub>c</sub> = 22.8 GAUSS



SLIDE 4

ZEEMAN TRANSITIONS IN O<sub>2</sub>

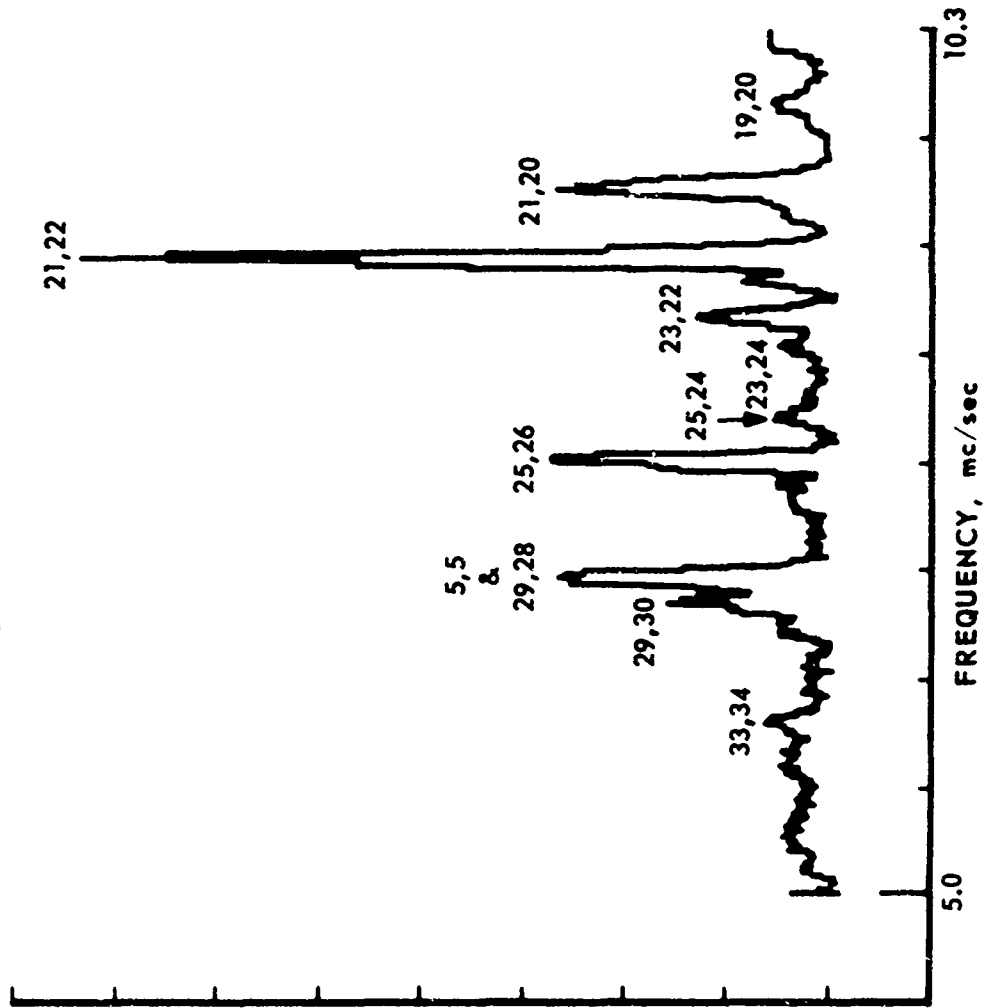
H<sub>c</sub> = 38.7 GAUSS



SLIDE 5

ZEEMAN TRANSITIONS IN O<sub>2</sub>

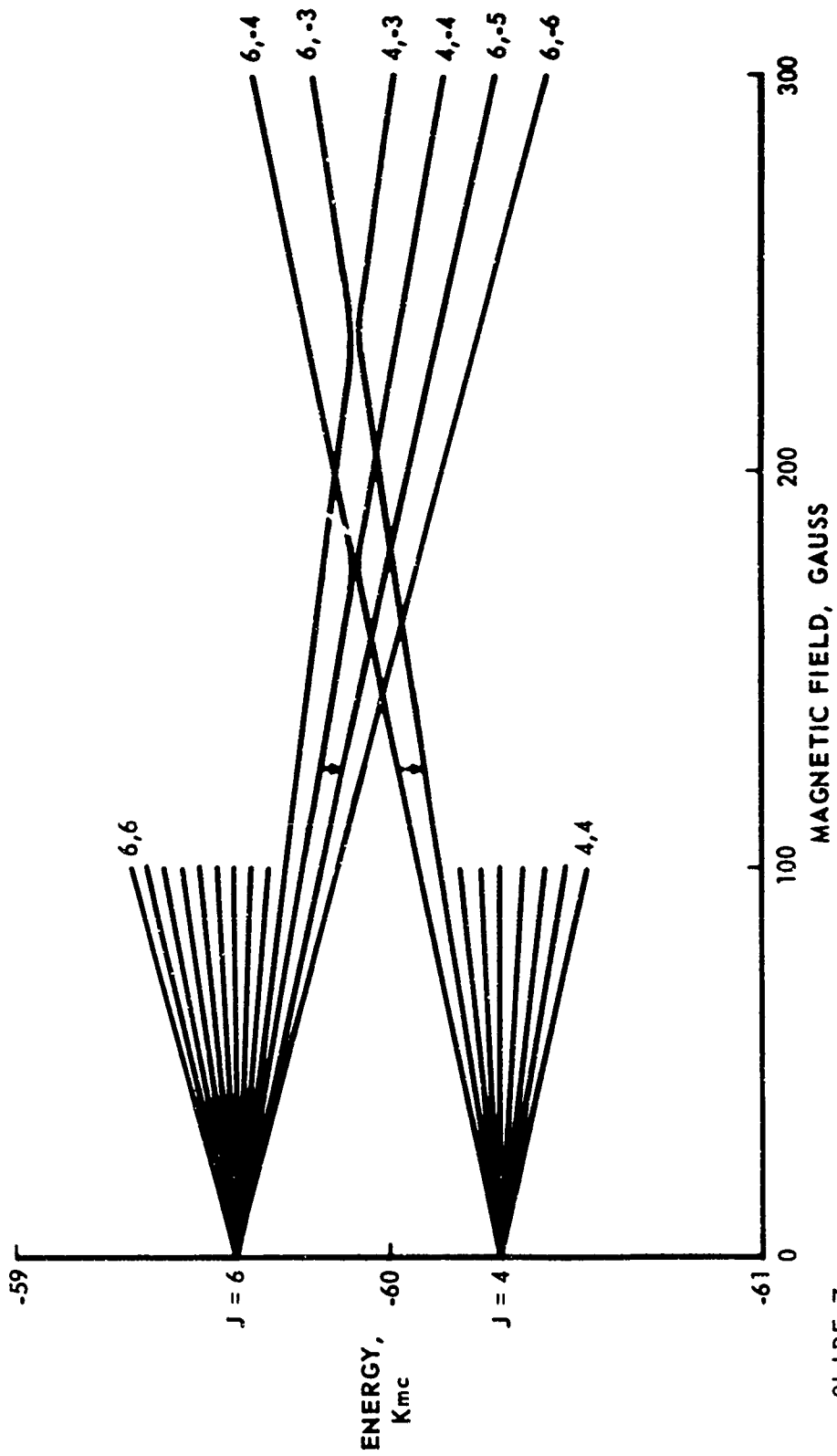
H<sub>c</sub> = 70.6 GAUSS



SLIDE 6

ENERGY LEVELS OF O<sub>2</sub>

K = 5



SLIDE 7

## APPENDIX B

### ELECTRON BOMBARDMENT MOLECULAR BEAM DETECTOR

Gilbert O. Brink

Cornell Aeronautical Laboratory, Inc.

#### ABSTRACT

A molecular beam electron bombardment detector is described and operational data are presented. The detector makes use of a Paul mass filter to increase its versatility. The detector is calibrated by the use of molecular beams of neon, argon, and krypton. Respective detection efficiencies are 1 atom in 2400, 320 and 80.

*Copy of paper published in Review of Scientific Instruments,  
37, 857 (1966).*



# ELECTRON BOMBARDMENT MOLECULAR BEAM DETECTOR<sup>\*</sup>

Gilbert O. Brink

Cornell Aeronautical Laboratory, Inc.

## INTRODUCTION

One of the major instrumental problems associated with molecular beam research is that of detecting the neutral beam in a quantitative manner. During the last few years much effort has gone into the development of detectors that ionize the beam by electron bombardment<sup>1-5</sup>. The ions thus produced are mass analyzed and the ion current measured by means of an electron multiplier. The mass analysis is usually carried out by means of a magnetic mass spectrometer.

There are a number of problems associated with a detector of this type. First of all it must be able to convert a reasonable fraction of the incident beam into detectable ions. Secondly, it must be capable of injecting these ions into the mass analyzer without excessive loss. Thirdly, the mass spectrometer must have a high transmission, a reasonable resolution, and not be too sensitive to such things as ion energy spread. It would also be convenient if the overall detector could be easily moved inside the vacuum housing.

The detector to be described here fulfills all of these conditions.<sup>6</sup> It operates on a principle similar to that used by Weiss<sup>4</sup> but differs in mechanical design. The mass analysis is carried out by means of a Paul mass filter<sup>7</sup> and this results in the instrument being more versatile than those using magnetic mass spectrometers. Although in the work described here the ion current was measured by means of a Faraday cup, an electron multiplier could easily be added to reduce the time constant and increase the sensitivity.

---

<sup>\*</sup>This work was internally supported by the Cornell Aeronautical Laboratory, Inc.

## DESCRIPTION OF THE DETECTOR

The instrument consists of three main parts: the ionizer, the mass filter and the ion collector. With the exception of the placement of the filament the entire instrument is symmetric about the molecular beam axis. The ionizer is surrounded by a grounded metal cylinder which serves as an electron reflector and radiation shield. A thorated tungsten filament is placed between this shield and a grid which operates at a positive potential so that electrons are accelerated through it. The general construction of the detector is shown in Figures 1 and 2.

This geometry results in the electrons oscillating many times through the molecular beam before they are ultimately collected by the grid. The effective electron current which is available to produce ionization in the molecular beam is therefore much greater than in any of the previously described detectors resulting in the observed high detection efficiency. This high electron current also produces a potential depression on the axis of the ionizer which effectively traps the beam ions and allows them to pass into the mass filter with minimal loss.

The four rods of the mass filter operate at a common potential a few volts less than that at the minimum of the potential well, thus reducing the ion energy to a value suitable for the operation of the mass filter. Since a Paul mass filter is not particularly sensitive to ion energy this common potential is not critical. The mass selected ions are extracted from the filter by means of a grounded aperture and focused into a collector cup. This cup could be replaced by an electron multiplier as mentioned above. A cup was used in this work to avoid the difficulties associated with the absolute measurement of multiplier gain.

The mass filter operates at a constant frequency of 1.00 mc/sec as determined by a crystal controlled oscillator. This oscillator drives a Class C RF amplifier which supplies the RF voltage for the rod system. This voltage can be varied by varying the plate voltage of the amplifier and mass is scanned

in this manner. The RF voltage is sampled, rectified, and the resulting DC fed to the rod system as shown in Figure 3. The ratio of this DC voltage to the RF voltage determines the resolution of the mass filter and this resolution can be adjusted at will by means of a panel control.

The ability to vary the resolution is a great advantage that this mass spectrometer possesses over the magnetic type. Since transmission and resolution are inversely related it is advantageous to use the minimum resolution necessary to suitably detect a given beam. Also since the majority of the background ions are of low mass, it is possible to operate this type of device as a high pass filter when detecting a heavy beam, thus taking advantage of low resolution and high transmission. It is also possible to use a second RF voltage to reject an interfering ion<sup>8</sup>.

The instrument is contained in a stainless steel vacuum housing and connected with the rest of the molecular beam apparatus by means of a small hole. The housing is entirely copper gasketed and is pumped by a liquid nitrogen baffled oil diffusion pump. With the ionizer operating the background pressure as read with a nude ionization gauge is about  $1 \times 10^{-9}$  Torr. The entire instrument mounts on a stainless steel plate which rolls on ball bearings and can be driven in a direction perpendicular to the beam axis from outside the vacuum housing, thus allowing the detector to be used to study beam shape.

#### OPERATION OF THE DETECTOR

In order to obtain good stability of the detector it is important that all of the applied potentials be well regulated. The grid potential of the ionizer is obtained from a John Fluke Model 407D power supply. The filament is heated with direct current from an emission regulator which samples the grid current and varies the heating current through the filament so that the electron emission current is kept constant. The RF power supply for the mass filter is also powered from a 407D power supply and no other regulation is needed. This supply has been modified so that the bias circuit supplies a positive accelerating potential for the rod system.

Typical operating conditions for the detector are shown in Table I. Although it is possible to obtain increased detection efficiency by raising the filament temperature the conditions given seem to permit maximum filament life. The detector appears to be stable over periods of several days and once it is set to a given mass number it need not be readjusted. The vacuum system is designed so that the detector remains on at all times and it is not let up to air except for maintenance.

Filament Current	4.2 amps
Grid Potential	+250 volts
Grid Current	125 ma
Common Rod Potential ( $V_{acc}$ )	+105 volts
Power Dissipated in Grid	31 watts
Background Pressure	$1 \times 10^{-9}$ Torr

Table I

#### CALIBRATION OF THE DETECTOR

The detector was calibrated by the use of molecular beams of neon, argon, and krypton whose absolute intensities were known. These intensities were obtained from a knowledge of the beam geometry and the rate of effusion from the beam source. Source pressures were measured by a thermocouple gauge which was calibrated against nitrogen by gas expansion from a known volume. The primary standard for the pressure measurements was a mercury manometer. The beam gas was continuously analyzed by means of a separate mass spectrometer and the total of all impurities is known to be below 10% for all gases used. The ion current was measured by a Keithley Model 417 electrometer.

## RESULTS

The results obtained with this detector are shown in Table II. The data represent a beam on - beam off measurement produced by a beam flag which physically interrupts the molecular beam. The resolution and the mass setting of the mass filter were adjusted to produce maximum detected signal. The potentials on the ionizer were also adjusted to maximize this signal. It is possible to detect the beams at lower efficiencies by operating the mass filter at higher resolution. This is useful in order to identify the species present in the beam. The resolution of the mass filter may then be lowered for general use as a detector. This is a feature that magnetic spectrometers do not possess.

Beam Gas	Mass Filter Operation	Input Beam Intensity, atom/sec	Ion Output Current, amp.	Detection Efficiency (Based on Singly Charged Ions)
Neon	$\frac{\Delta m}{m} \approx \frac{1}{4}$	$6.4 \times 10^{10}$	$4.3 \times 10^{-12}$	1 atom in 2400
Argon	$\frac{\Delta m}{m} \approx \frac{1}{5}$	$2.5 \times 10^{10}$	$7.0 \times 10^{-12}$	1 atom in 600
Argon	High Pass Filter	$2.4 \times 10^{10}$	$1.2 \times 10^{-11}$	1 atom in 320
Krypton	High Pass Filter	$1.2 \times 10^{10}$	$2.3 \times 10^{-11}$	1 atom in 80

Table II

## DISCUSSION

It is apparent from the preceding data that this detector is capable of detecting a molecular beam with high efficiency. This efficiency appears to be a direct consequence of the cylindrical geometry and the resulting effective electron current. As with other electron bombardment detectors the efficiency in any particular case is dependent on the temperature of the beam and the ionization cross sections of the species present in the beam. Thus the actual numerical values presented here should be taken as representative of the type of operation that may be obtained with this detector.

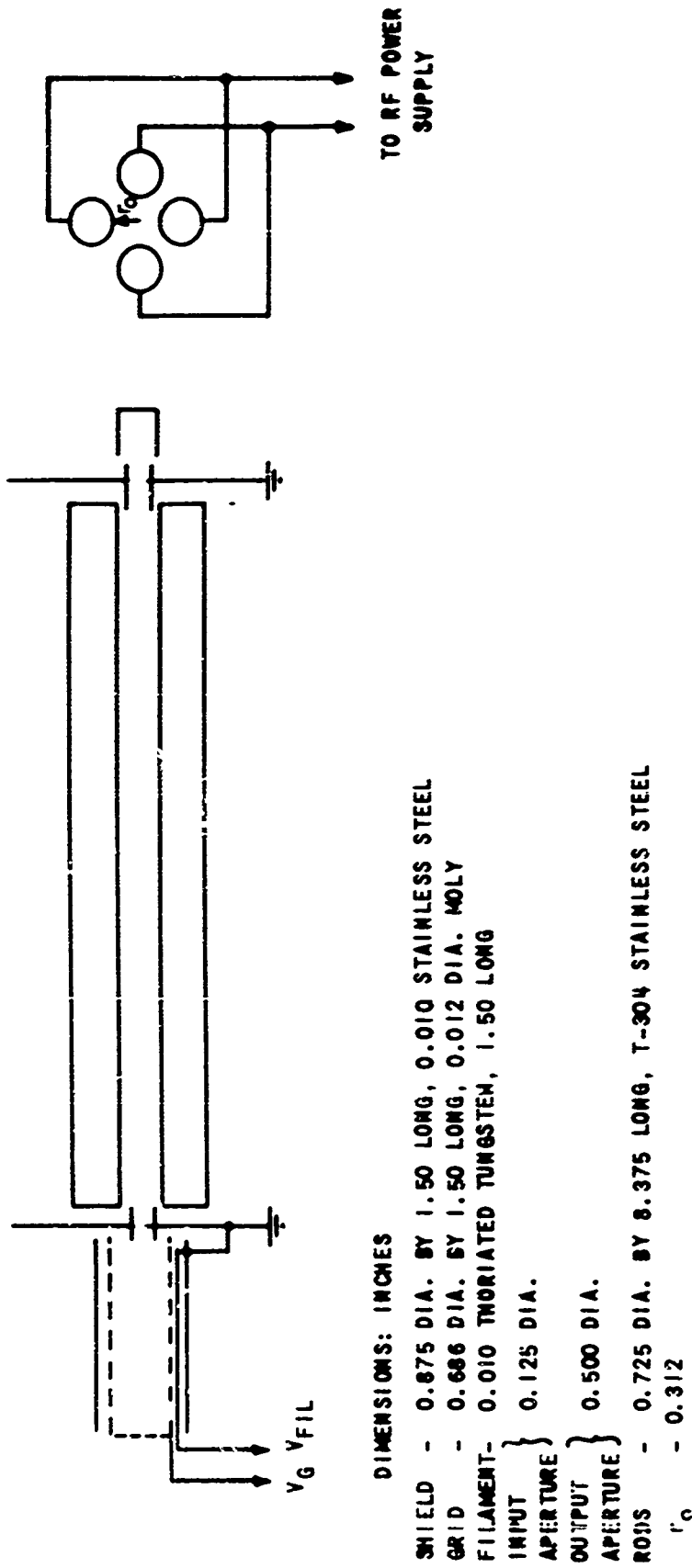
The ability to vary the resolution of the detector at will allows the detection efficiency to be optimized for a given beam. In the case of an interfering ion a second RF voltage may be applied to reject the interfering species and the resolution of the detector need not be increased. Thus it is possible to operate at high transmission and still obtain a good signal-to-noise ratio.

### ACKNOWLEDGMENTS

The author is grateful to Dr. D. P. Malone for helpful discussions and assistance in the taking of data. Thanks are also due to Mr. R. A. Fluegge for the construction of the gas handling system, assistance in its calibration, and analysis of the beam gases. Dr. George Skinner of the Aerodynamics Department assisted in the support of this work. Much of the mechanical work was done by James Huber and the staff of the Physics Division Machine Shop.

### REFERENCES

1. G. Wessel and H. Lew, Phys. Rev. 92, 641 (1953)
2. G. Fricke, Z. Physik, 141, 166 (1955)
3. W. E. Quinn, A. Pery, J. M. Baker, H. R. Lewis, N. F. Ramsey and U. T. LaTourrette, Rev. Sci. Instr. 29, 935 (1958)
4. R. Weiss, Rev. Sci. Instr. 32, 397 (1961)
5. H. G. Bennewitz and R. Wedemeyer, Z. Physik, 172, 1 (1963)
6. Preliminary results concerning the operation of this type of detector were presented at the Seventh "Brookhaven" Conference on Molecular Beams and Atomic Resonance, University of Uppsala, Sweden, 1964, and at the Los Angeles meeting of the American Physical Society, December 20-22, 1965.
7. W. Paul and M. Raether, Z. Physik, 140, 262 (1955)
8. W. Paul and H. P. Reinhard, Proc. Symposium on Isotope Separation, Amsterdam, (1967)



The ionizer was constructed from an EAI Model 606 Electron Gun Kit, manufactured by Nuclide Corp., Medford, Mass.

Figure 1 GEOMETRY OF MOLECULAR BEAM DETECTOR

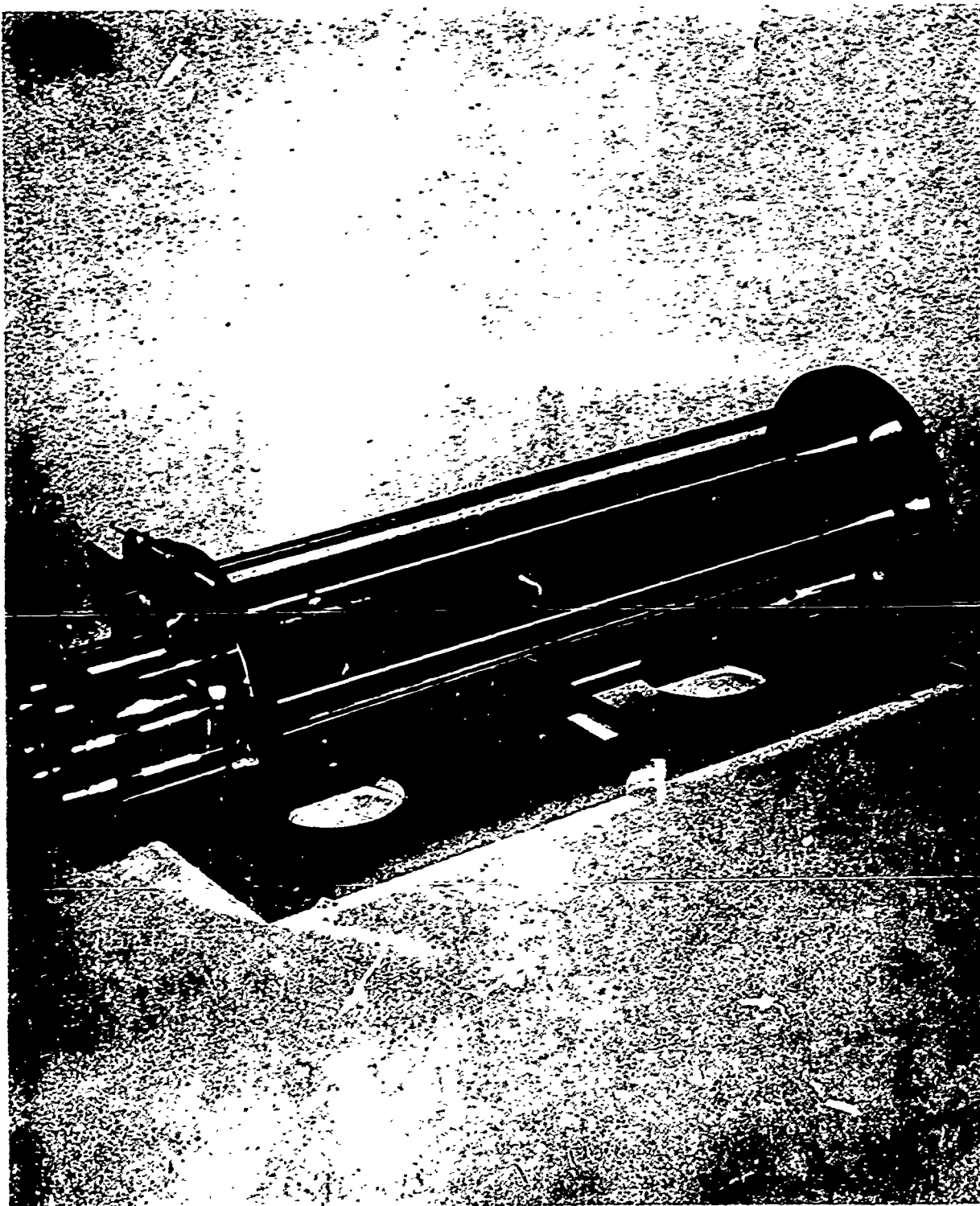
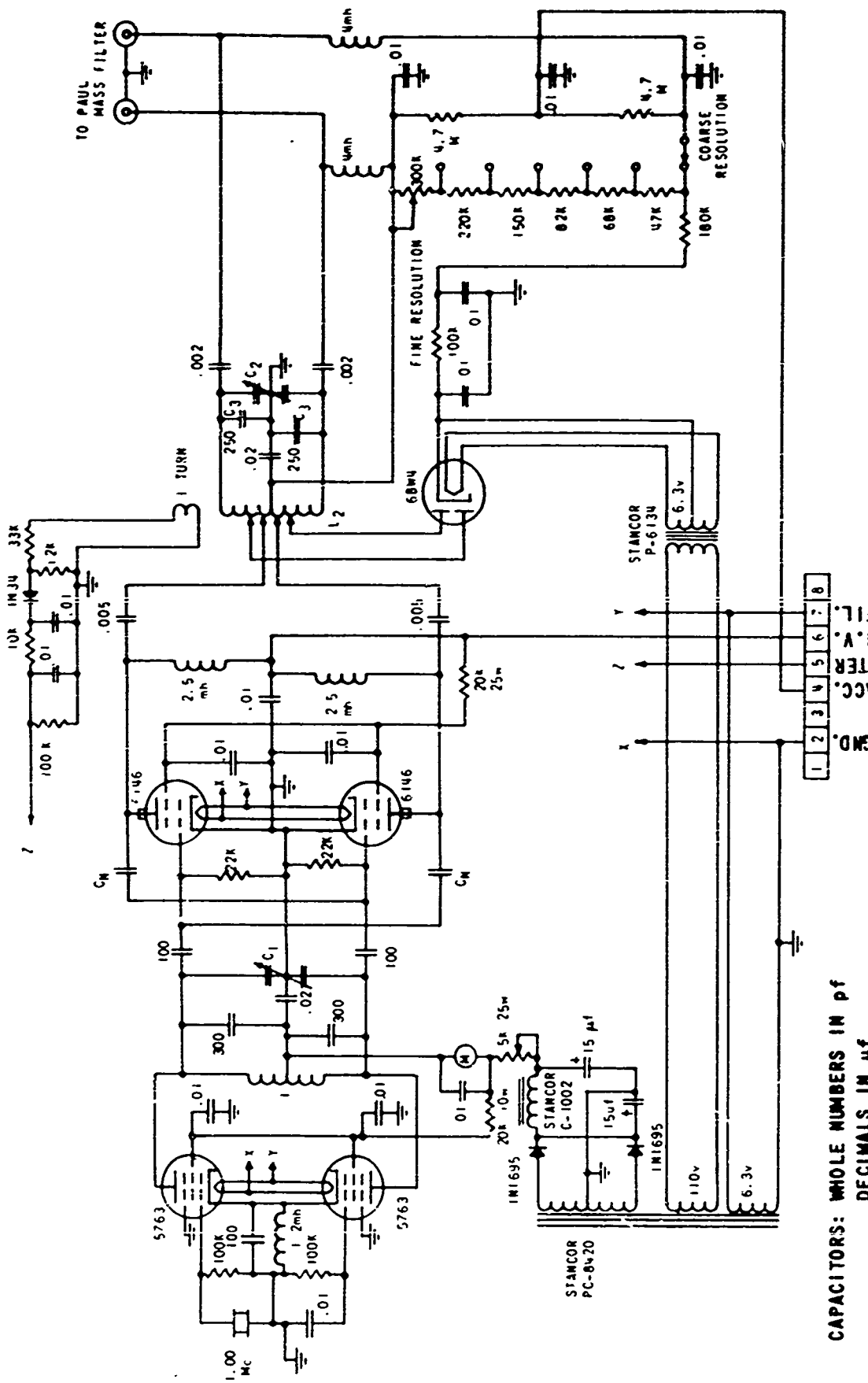


Figure 2 MOLECULAR BEAM DETECTOR





- L<sub>1</sub> - MILLEN TYPE 43161
- L<sub>2</sub> - 42 TURNS, 6-1/2 IN. LONG BY 6 IN. DIA.
- M - 0-100 Ma
- C<sub>1</sub> - MILLEN TYPE 23140 TM
- C<sub>2</sub> - MILLEN TYPE 04200
- C<sub>3</sub> - VACUUM CAPACITOR, JENNINGS JC5L-250-3KV

CAPACITORS: WHOLE NUMBERS IN pf  
 DECIMALS IN  $\mu$ f  
 RESISTORS: 1 WATT EXCEPT WHERE NOTED

Figure 3 MASS FILTER POWER SUPPLY